AD NUMBER
AD375686
CLASSIFICATION CHANGES
TO: unclassified
FROM: confidential
LIMITATION CHANGES
TO: Approved for public release, distribution unlimited
FROM: Distribution authorized to U.S. Gov't. agencies and their contractors; Administrative/Operational Use; 15 SEP 1966. Other requests shall be referred to Army Missile Command, Redstone Arsenal, AL.
AUTHORITY
30 Sep 1978, DoDD 5200.10; MICOM ltr, 1 Feb 1979

SECURITY MARKING

The classified or limited status of this report applies to each page, unless otherwise marked.
Separate page printouts MUST be marked accordingly.

THIS DOCUMENT CONTAINS INFORMATION AFFECTING THE NATIONAL DEFENSE OF THE UNITED STATES WITHIN THE MEANING OF THE ESPIONAGE LAWS, TITLE 18, U.S.C., SECTIONS 793 AND 794. THE TRANSMISSION OR THE REVELATION OF ITS CONTENTS IN ANY MANNER TO AN UNAUTHORIZED PERSON IS PROHIBITED BY LAW.

NOTICE: When government or other drawings, specifications or other data are used for any purpose other than in connection with a definitely related government procurement operation, the U. S. Government thereby incurs no responsibility, nor any obligation whatsoever; and the fact that the Government may have formulated, furnished, or in any way supplied the said drawings, specifications, or other data is not to be regarded by implication or otherwise as in any manner licensing the holder or any other person or corporation, or conveying any rights or permission to manufacture, use or sell any patented invention that may in any way be related thereto.

CONFIDENTIAL

COPY NUMBER 6

Report No. S-80

BURNING RATES OF SOLID COMPOSITE PROPELLANTS AT PRESSURES UP TO 20,000 psig (U)

U. S. ARMY MISSILE COMMAND

This document contains information affecting the national defense of the United States within the meaning of the Espionage Laws, Title 18, U.S.C., Sections 793 and 794. The transmission or the revelation of its contents in any manner to an unauthorized person is prohibited by law.

DOWNGRADED AT 3 YEAR INTERVALS:
DECLASSIFIED AFTER 12 YEARS.
DOD DIR 5200.10

ROHM AND HAAS
REDSTONE RESEARCH LABORATORIES
HUNTSVILLE, ALABAMA 35807

CONFIDENTIAL

DISCLAIMER NOTICE

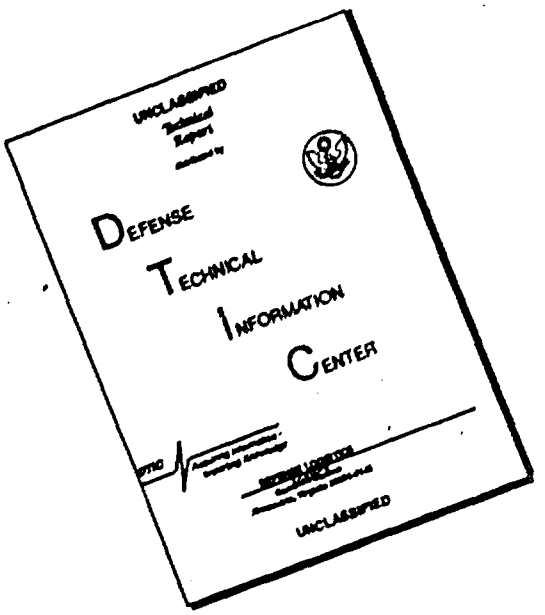

THIS DOCUMENT IS BEST QUALITY AVAILABLE. THE COPY FURNISHED TO DTIC CONTAINED A SIGNIFICANT NUMBER OF PAGES WHICH DO NOT REPRODUCE LEGIBLY.

CONFIDENTIAL

ROHM AND HAAS COMPANY

REDSTONE RESEARCH LABORATORIES
HUNTSVILLE, ALABAMA 35807

Report No. S-80

BURNING RATES OF SOLID COMPOSITE PROPELLANTS AT PRESSURES UP TO 20,000 psig (U)

by

R. B. Cole

Approved:

September 15, 1966

Louis Brown, Head
Ballistics Section

Contract Number:
DA-01-021 ORD-11909(Z)

O. H. Loeffler
General Manager

CONFIDENTIAL

NOTE ON CLASSIFICATION

The entire text of this report is Unclassified, except for Table II, p. 14. The Figures are Unclassified when separated from the "Propellant Index to Figures" and when those parts of the captions in brackets, [ ], are deleted.

ROHM AND HAAS COMPANY

REDSTONE RESEARCH LABORATORIES
HUNTSVILLE, ALABAMA 35807

BURNING RATES OF SOLID COMPOSITE PROPELLANTS AT PRESSURES UP TO 20,000 psig

ABSTRACT

Strand burning rates of ammonium perchlorate-containing composite propellants having plastisol-nitrocellulose, carboxyl-terminated-polybutadiene, and NF binders have been measured to 20,000 psig. For the first two types and probably the NF type the major influences on burning-rate transition are those resulting from variations in binder type and in oxidizer concentration and particle size; the presence of aluminum or burning-rate promoters has little effect on the pressure-dependence of the burning rate at high pressure. The pressure exponents of plastisol-nitrocellulose formulations reach constant values of 1.0 to 1.3 at about 6000 psi, with little dependence on AP particle size. Carboxyl-terminated-polybutadiene formulations examined give indexes from 0.3 at 2000 psi to 2 up to 10,000 psi, with appreciable AP-particle-size dependence; above 10,000 psi the index decreases to 0.9 and appears to be insensitive to oxidizer size. A proposed model suggests an alteration in the volatilization processes which ensue from differences in pressure-dependence of the respective binder and oxidizer release rates.

ACKNOWLEDGEMENTS

The author wishes to acknowledge the helpful cooperation of Mr. S. E. Anderson in the processing of propellant samples and his substantial contribution in supplying comparison data from motor firings, of Dr. W. A. Wood and Dr. R. H. W. Waesche in discussion of diverse aspects of the work and in review of the manuscript, and of Mr. P. H. Gehlhaus in his advice on the installation and operation of the strand burner.

TABLE OF CONTENTS

Table of Contents (Continued)

LIST OF FIGURES

Figure

ROHM AND HAAS COMPANY

REDSTONE RESEARCH LABORATORIES
HUNTSVILLE, ALABAMA 35807

BURNING RATES OF SOLID COMPOSITE PROPELLANTS AT PRESSURES UP TO 20,000 psig

INTRODUCTION

In recent years, specific mission requirements for solid-propellant rockets have led to increased consideration of rocket-chamber pressures in the range of 2000 to 10,000 psi. An obstacle to the successful design of such high-pressure motors is the fact that numerous solid-propellant formulations found satisfactory at lower chamber pressures exhibit a transition to a high pressure index, n, in the 3000-to-6000-psi region.

Propellants for which transition has been observed have been of the heterogeneous type and include both conventional inert-binder composite (1)* and plastisol-nitrocellulose composite formulations (2). An indication of such behavior has also been found with NF-binder composite propellants (3). Common to all of the propellant systems in which these burning-rate transitions have been observed is the presence of ammonium perchlorate (AP) as oxidizer. Even pure AP in pressed strands has exhibited an

*Numbers in parentheses indicate references on p. 36.

abrupt transition to high index ($n \cong 1.75$) at 5000 psi (4), (5), (6). On the other hand, it has been reported by several sources that neither potassium perchlorate-oxidized propellants nor homogeneous double-base propellants undergo pressure-index transition up to 20,000 psi (5), (7), (8), (9).

The interpretation of most prior results involving propellant-composition influences on transition is complicated by the change of several variables at once in the course of the experimental program. It has been reported that the addition of catalysts to propellants displaces the beginning of transition to higher pressure levels and that oxidizer size has little effect on the pressure level at which transition begins (10), (11). These and similar observations are not, however, made in situations which allow a clear separation of the various possible compositional influences on transition by propellant composition. The reason for this is that the data have usually been derived from propellant-development programs rather than from studies aimed specifically at investigation of the transition phenomenon itself.

Two hypotheses of the transition of pure ammonium perchlorate have been suggested. The more fully developed, analytically, of the two, a "porous-burning" theory (4), (5), (12), remains essentially untested, except in the sense that it accounts for the results of the small number of experimental observations which led to its conception. Although transition phenomena appear consistent with this theory (or, at least, cannot be proven to be inconsistent), applicable experimental data are scant. The second hypothesis of transition has not been reported in great detail. It hinges on the notion of interfacial "flashing" of burning from one oxidizer particle to the next ("successive ignition") (13), (14). There are no experiments reported which have been carried out with the specific aim of testing the validity of either theory.

SCOPE OF INVESTIGATION

The purpose of this investigation is the elucidation of the parametric influences on the physical or chemical nature (or both) of burning-rate transition at high pressure. Heterogeneous ammonium perchlorate-oxidized composite propellants of both conventional (inert) binder and plastisol-nitrocellulose binder are considered as well as a few NF formulations. The experimental program is divided into two parts, each directed at a different aspect of transition. The major part is aimed at providing an empirical characterization of the dependence of high-pressure burning rates and transition on propellant composition factors such as oxidizer-particle size, binder type, additive content, etc. It involves strand-burning-rate measurements at pressures between 2000 and 20,000 psig for several representative propellant formulations.

The other part consists of diagnostic experiments bearing on the mechanism of transition. The principal technique used was high-speed photography of propellant burning at pressures above and below the onset of transition. Fracture of ammonium perchlorate under the action of thermal stress was also examined.

Finally, a phenomenological model of composite-propellant combustion is sketched which is consistent with the body of data obtained.

STRAND-BURNING-RATE MEASUREMENT

Since the first step toward meaningful consideration of transition phenomena must be the determination of trends in burning or regression rate (r) vs. pressure (P) and compositional influences on them for propellants exhibiting transition, an experimental program was carried out to measure the burning rates of several solid-propellant formulations at pressures between 2000 and 20,000 psig. For the most part, r—P data were obtained by burning $\frac{1}{8}$-in. octagonal strands (across flats) about $3\frac{5}{8}$ inches long. The strands were usually burned while submerged in oil, and regression rates were determined from the time interval between the melting of two transverse fuse wires set in holes drilled in the strands 3 inches apart.

Selection of Technique

Useful and common techniques for low-pressure ("pre-transition") burning-rate determination include firings in small rocket motors, vented strand burners, or closed strand burners (15). Owing to the occurrence of pressure indexes exceeding unity, as a consequence of transition, and to the instability of rocket motors under such conditions, little consideration was given to motor firings except as a source of low-pressure comparison data. Although pressure-regulator-vented burners can be readily used at low pressures, the unavailability of commercial pressure regulators operable between 5000 and 20,000 psig made the use of vented strand burners unsuitable for transition studies. Thus, by elimination, the only practical means for determining r—P trends at high pressure, particularly in the transition regime, is a closed or Crawford-type strand burner. While the absolute magnitudes of burning rates measured in such burners are not identical with those from rocket-motor firings, the r—P trends observed are, in general, the same (16), (17).

The technique of burning a small strand of propellant in a closed chamber offers two routes to burning-rate measurement. The rate of burning may be determined either directly, by measuring burning-surface displacement with time by use of fusible timing wires, thermoelectric sensors, microwave Doppler-shift analysis, etc., or indirectly, by inferring mass burning rate from rate of pressure rise (dP/dt) in the chamber. The latter method suffers from the uncertainty both as to the product-gas equation of state and as to the existence of gas equilibrium, and was therefore eliminated. On the other hand, the well-tried fusible-timing-wire technique for surface-displacement—time measurement is less uncertain and is as practical at high pressures as at the lower pressures where it has commonly been used; hence, it was selected for observing r—P relations in the transition and post-transition regimes.

Having settled on the closed-burner technique, consideration was given to the question of pressure rise during burning. Since fusible timing wires, for example, measure an elapsed time for burning to traverse a predetermined length, the accuracy of rate determination is sensitive to changes in rate resulting from pressure change during the burning. This pressure change is primarily a function of the strand size, propellant type, burner configuration, and of the mass and composition of the chamber gas present before ignition. The fractional increase in pressure during burning may be expected to be of the order of the product of the ratios of the propellant mass to the original chamber gas mass and the propellant flame temperature to the initial chamber gas temperature $\left(\Delta P \cong \frac{m_p}{m_o} \cdot \frac{T_f}{T_o}\right)$. For firings near room temperature, the temperature ratio is of the order of 10; therefore, moderately low pressure increases of, say, 10% may be achieved only by the use of relatively large chamber-gas masses 10 to 100 times the propellant sample mass.

The pressure rise accompanying the firing of a closed strand burner can be reduced by submerging the strand in a liquid, with only a small free volume above the liquid. Water or light oil is a convenient, economical medium for this purpose; both have been shown to affect the propellant burning rate only negligibly, at the same time reducing pressure rise and, in many cases, eliminating the necessity for restricting strand sides to prevent "flash" burning (18), (19). The smaller pressure rise resulting from the burning of propellant under oil or water decreases the volume of initial gas required in the strand burner to minimize pressure rise during burning. This decrease in volume (or mass) obviously decreases the compressive work required to prepressurize the strand burner before firing. Since compression of either gases or liquids to pressures approaching 20,000 psig is typically accomplished using positive-displacement pumps, any decrease in the mass of initial gas required for strand-burner operation allows an appreciable decrease either in the pump size or in the pumping time required for prepressurization. For these reasons, a closed, liquid-filled strand burner was used for regression-rate determinations.

Apparatus

20,000-psig Strand Burner - An existing unit was used for the strand-burning experiments of this investigation. Basically the burner was a cylindrical commercial reactor, $5\frac{1}{2}$ inches O.D. × $21\frac{1}{2}$ inches long, mounted vertically and having a 1.3-ℓ cylindrical cavity $2\frac{1}{2}$ inches in diameter × $16\frac{5}{6}$ inches long. The reactor was equipped at the top with an O-ring-seal tapered plug loaded by a mating nut which screwed into buttress-type threads at the top of the reactor. A $\frac{5}{8}$-in. cone-type high-pressure-tubing tap was provided at the bottom end of the reactor. The external cylindrical surface of the reactor was surrounded by an 8-in.-O.D. soft-metal (lead–tin alloy) casting containing

twelve 350-watt cartridge-type resistance heaters. The casting also contained a refrigeration-system evaporator in the form of a 38-ft. coil of $\frac{3}{8}$-in.-O.D. copper tubing. A copper—constantan thermocouple was also located within the soft-metal casting. The outside diameter of the casting was surrounded by 2 inches of insulating fill (vermiculite). The complete assembly of reactor, casting, and insulation was mounted within a steel housing $12\frac{3}{4}$ inches in diameter; the housing in turn was mounted on floor pedestals (Fig. 1).

The tapered plug which closed the top opening in the strand burner was equipped with five electrical lead-throughs, for igniter- and timing-wire leads, and a thermocouple well (Figs. 2 and 3). The electrical lead-throughs utilized conical load plugs designed to provide unsupported-area-type sealing, with Teflon insulators between the surfaces of the load plugs and the tapered plug. From the inside face of the tapered plug, long stainless-steel electrodes and a clamp rod for holding the propellant sample extended into the interior of the reactor. The thermocouple well, which contained a copper—constantan thermocouple, also extended into the cavity interior. On the outside of the firing head, electrical connectors led to cables which ran between the test cell and the control room.

Temperature control of the strand burner was accomplished by a recording temperature controller which provided on—off control of the twelve resistance heaters incorporated in the burner assembly. Nine of these heaters had manually set levels, six through a 20-amp autotransformer. The other three heaters were provided only with manual on—off control. The temperature-controller operation was governed by the thermocouple within the soft-metal casting. For low-temperature operation, a one-ton refrigeration system using the built-in evaporation coil of the strand burner was operated continuously and the heaters were used for control.

Pressurization System - An oil-and-bottled-nitrogen pressurization system (Fig. 4) was used to achieve a test pressure of 20,000 psig with the strand submerged in light oil. The burner was pressurized before firing and vented after firing through $^{9}/_{16}$-in.-O.D. high-pressure tubing connected to the bottom of the reactor. A manifold and valves connected to this tubing allowed prepressurization of the burner with nitrogen to 1000 to 2000 psig, oil-displacement compression of this nitrogen to the desired operating pressure, and subsequent venting of the product-gas—nitrogen mixture and oil to a dump can. A 25,000-psig-rupture-disc assembly on the manifold guarded against overpressurization.

The source of nitrogen for pressurization was a manifolded bank of three water-pumped-nitrogen-gas bottles. Oil-displacement pumping was accomplished with two piston-type hydraulic pumps in tandem to give a total pumping capability of 1.1 gal./hr. The oil-supply system was also protected by a 25,000-psig-rupture-disc assembly. Two standard Bourdon-type gauges (calibrated 0 to 10,000 psi and 0 to 40,000 psi) provided monitoring of the chamber-prepressurization and oil-pumping processes; a third gauge indicated the nitrogen-manifold pressure. All gauges and valves were located in a control room shielded from the test cell.

Instrumentation - Instrumentation for pressure and burning-rate measurement included:

(1) a diaphragm-type, bonded-strain-gauge pressure transducer (0 to 20,000 psig nominal range) with an amplifier, double-shunt four-step calibrator, power supply, and a Sanborn Model 60-1300B recording oscillograph;

(2) a strand timer and igniter unit providing clock timing of the interval between melting of two fuse wires (accurate to 0.01 sec) and a 0-to-18-V a.c. power supply for a hot-wire igniter;

(3) a second channel on the oscillograph to record the time interval between fuse-wire meltings;

(4) a potentiometer for monitoring the temperature of the strand-burner oil bath in which the propellant sample was submerged prior to firing. Ordinarily the reading was taken from the thermocouple firing head. However, in some ambient- and elevated-temperature firings, the temperature-controller thermocouple located in the soft-metal casting was used.

A schematic diagram of the strand-burner instrumentation is shown in Fig. 5.

The strand timer was of a design used previously (18), in which the open circuits caused by melting of the fuse wires triggered thyratrons, closing relays which engaged and disengaged the clutch of the interval-timing clock. The clock dial was subdivided into increments of 0.01 sec.

The fuse-wire signals were also fed to the oscillograph which, together with known-interval timing marks automatically provided on the record, allowed data reduction from a single oscillographic record displaying pressure history during firing, pressure-calibration steps, and the time interval between melting of the two fuse wires. The record also allowed determination of the pressures at the beginning and end of the timed interval of burning to obtain an average pressure during the interval. This is an improvement over some previous closed-bomb studies in which combustion pressure must be calculated from the initial and peak pressures observed during burning (18).

Precision of Measurements

The observed quantities involved in determining the r—P data of this study were:

(1) the axial separation of the two fuse wires transverse to the strand, Δx,

(2) the time interval between melting of the two fuse wires, Δt,

(3) the pressures at melting of the first and second wires, P_1, P_2.

The reported r—P data were based on calculations from these quantities from the relations:

$$r = \frac{\Delta x}{\Delta t} \tag{1}$$

$$P = \frac{P_1 + P_2}{2} \tag{2}$$

With rare exceptions, in most of the strand-burning experiments of this study Δx was fixed at 3.00 ± 0.02 inches; hence, the maximum error in Δx was less than 1%. The maximum error in determination of Δt depended on its value, which varied from 0.20 to 10.0 sec for the 3.00-in. fuse-wire spacing and the range of regression rates encountered. Since the maximum error in time measurement was less than 0.01 sec, the maximum error in Δt was between 0.01 % and 5%. For the shortest burning times (0.30 sec) at the highest pressure and with the fastest-burning propellant, it was possible to decrease the maximum error in burning time below 5% by using a CRT oscilloscope to record the interval instead of the clock.

The maximum error in burning-rate determination depended, of course, on factors in addition to those in time and distance measurement. Such factors were the occurrence of tilted or nonplanar burning surfaces and composition variations within a given propellant sample owing to oxidizer settling, incomplete mixing, normal variations in composition during formulation, etc. The potential magnitude of such factors was not specifically checked except for routine density measurements made on each propellant batch. However, excellent strand-to-strand and batch-to-batch reproducibility was evident in check-out firings.

Errors in combustion-pressure measurement may be attributed to several sources, e.g., failure of the pressure transducer to "track", error in transducer calibration, recorder and amplifier non-linearities, poor precision in reading transducer output from the oscillographic record, and also the necessity of averaging a changing pressure to find an effective combustion pressure. The first two sources were neglected in view of the excellent calibration data obtained, the proximity of the transducer to the test chamber, the relatively low rates of pressure rise measured during burning (16,000 psi/sec maximum), the existence of an essentially incompressible liquid medium between the strand and the pressure transducer, and the very small mass flows required to effect response by the diaphragm-type pressure transducer.

Error due to recorder and amplifier non-linearities were probably small, since the recorder was used in the center 3 cm of its 5-cm galvanometer range. In this center range, the recorder system response (including built-in amplifier and galvanometer) was specified by the manufacturer to be linear to within ± 0.50 mm. The maximum recording sensitivity used in the experiments of this investigation was approximately 300 psi/mm; hence, the maximum error in pressure recording was about 150 psi. However, the recording sensitivity used for the lowest-pressure firings (2000 psig) was such as to give a maximum error of about 100 psi. Therefore, maximum errors in pressure recording ranged from about 5% at 2000 psig to 0.7% at 20,000 psig.

Error in reading indicated pressures from the recorder chart was estimated to be less than 0.2 mm, which corresponded to pressure errors from 2% at 2000 psig to 0.3% at 20,000 psig.

The time-varying pressure of closed-strand-burner firings necessitated assigning a single, quasi-steady combustion pressure characteristic of the firing. This pressure should ideally equal that which would have resulted in the average burning rate determined from Eq. 1. Thus

$$r = \frac{\Delta x}{\Delta t} = f[P(t)] = F[P_{eff}]$$

where f is an integral function depending on the pressure history, $P(t)$, but numerically equal to the normal burning-rate-pressure function, F, evaluated at a single "effective" pressure, P_{eff}, within the pressure range of the experiment. As shown in the Appendix, a satisfactory approximation in cases of this type is simply the arithmetic mean of the initial and final pressures.

$$P_{eff} = \frac{P_1 + P_2}{2}$$

Table I summarizes the maximum expected error in the r—P data of this investigation.

Table I

Summary of Estimated Maximum r—P Measurement Errors

Regression Rate (r)	
Distance burned (Δx)	<0.6%
Time of burning (Δt)	<0.01 to 5.0%[a]
	<0.7 to 5.6%[a]
Pressure (P)	
Transducer calibration	<1%
Recording-system non-linearity	<5.0 to 0.7%[a]
Recorder-chart reading	<2.0 to 0.3%[a]
Time-varying pressure (pressure averaging)	<0.1%
	<8.1 to 2.1%[a]

[a]Estimated values at 2000 psi and 20,000 psi combustion pressures, respectively.

Propellant Selection

To characterize the transition for the main classes of heterogeneous solid propellants, one inert-binder- and two reactive-binder-composite-propellant types were studied (Table II). r—P data for these formulations allowed examination of the effects of diverse composition variables on transition.

Table II

Thermochemical Data and Compositions of Propellants

Constituent, wt. %	Plastisol-Nitrocellulose Propellants							Inert-Binder (Carboxyl-Terminated-Polybutadiene Propellants)						NF Propellant
	RH-P-112	RH-P-181	RH-P-408	RH-P-402	RH-P-403	RH-P-404	Binder	RH-C-40	RH-C-41	RH-C-46	RH-C-49	RH-C-42	RH-C-43	RH-SB-103
Double-Base Powder[a]	16.7	19.6	15.2	12.5	19.4	19.4	30.9	----	----	----	----	----	----	----
TEGDN[b]	37.3	43.9	33.9	51.0	43.5	43.5	69.1	----	----	----	----	----	----	----
Resorcinol	1.0	1.2	0.9	1.2	1.2	1.2	----	----	----	----	----	----	----	----
Ammonium Perchlorate[c]	30.0	35.3	50.0	35.3	35.0	35.0	----	75.0	80.0	60.0	68.1	74.3	74.3	46.0
H-C[d] Polymer	----	----	----	----	----	----	----	17.9	13.2	28.7	16.3	17.7	17.7	----
DOA[e]	----	----	----	----	----	----	----	7.0	6.7	11.2	6.4	6.9	6.9	----
Iron Linoleate	----	----	----	----	----	----	----	0.1	0.1	0.1	0.1	0.1	0.1	----
NFPA[f]	----	----	----	----	----	----	----	----	----	----	----	----	----	13.0
TVOPA[g]	----	----	----	----	----	----	----	----	----	----	----	----	----	26.0
Aluminum[h]	15.0	----	----	----	----	----	----	----	----	----	9.1	----	----	15.0
Copper Chromite[i]	----	----	----	----	----	0.9	----	----	----	----	----	----	1.0	----
Lead Chromate[j]	----	----	----	----	0.9	----	----	----	----	----	----	----	----	----
Ferrocene[k]	----	----	----	----	----	----	----	----	----	----	----	1.0	----	----
Flame Temp.[l] (° K)														
@1000 psia	3384[P]	2680	2996	2597	----	----	----	1731	2263	<1361	2382[P]	----	----	3666[P]
@20,000 psia	3523[P]	2700	3099	2611	----	----	----	1814	----	1525	2404[P]	----	----	----
Molecular Wt,[m]														
@1000 psia	26.8[P]	24.0	26.0	23.4	----	----	----	20.0	22.3	<19.1	21.8[P]	----	----	24.4[P]
@20,000 psia	27.2[P]	24.0	26.3	23.5	----	----	----	20.6	----	20.7	21.9[P]	----	----	----
Specific Impulse[n] (lbf-sec/lbm)														
@1000 psia	258.7[P]	238.4	247.7	236.4	----	----	----	207.6	225.1	<209.3	231.1[P]	----	----	270.8[P]
@20,000 psia	306.4[P]	279.4	290.3	277.7	----	----	----	255.4	----	236.3	275.9[P]	----	----	----

[a] Fluid Ball Powder, Type B; Olin Mat[illegible] Cl[illegible]

@20,000 psia	27.2[p]	24.0	26.3	23.5	----	----	----	20.6	----	20.7	21.9[p]	----	----	----
Specific Impulse[n] (lbf-sec/lbm)														
@1000 psia	258.7[p]	238.4	247.7	236.4	----	----	----	207.6	225.1	<209.3	231.1[p]	----	----	270.8[p]
@20,000 psia	306.4[p]	279.4	290.3	277.7	----	----	----	255.4	----	236.3	275.9[p]	----	----	----

[a] Fluid Ball Powder, Type B; Olin Mathieson Chemical Company
[b] Triethylene glycol dinitrate
[c] With 1% tricalcium phosphate anti-caking agent
[d] 95.1% carboxyl-terminated polybutadiene polymer (ZL-434; Thiokol Chemical Corporation, Trenton, New Jersey)
3.6% MAPO (tris[1-(2-methyl)aziridinyl] phosphine oxide; International Chemical Corporation, Newark New Jersey)
1.3% ERLA(trifunctional epoxide; Bakelite Division of Union Carbide Chemical Corporation, New York, New York)
[e] Dioctyl adipate
[f] Copolymer of 2, 3-bis(difluoramino)propyl acrylate and hydroxypropyl methacrylate
[g] 1, 2, 3-tris[1, 2-bis(difluoramino)ethoxy] propane
[h] 6-8μ d_m; Alcoa 140, Aluminum Company of America, Pittsburgh, Pa.
[i] Cu0202, Harshaw Chemical Company, Cleveland, Ohio
[j] Reagent Grade, Fisher Scientific Company, Pittsburgh, Pa.
[k] Reagent Grade, Arapahoe Chemical Company, Boulder, Colorado
[l] Equilibrium adiabatic flame temperature
[m] Mean molecular weight of equilibrium product gases
[n] Propellant specific impulse with equilibrium flow to 14.7 psia
[p] With liquid Al_2O_3 in exhaust

A propellant already studied in great detail, RH-P-112, was chosen to check out the strand burner and its instrumentation, the pressurization system, firing procedure, etc. An unaluminized form of RH-P-112 was selected as the control or reference plastisol-nitrocellulose (NC) propellant. Although elimination of aluminum made this latter propellant, RH-P-181, unattractive in terms of ballistic performance, it simplified subsequent theoretical and analytical considerations of combustion mechanism. RH-P-181 was then varied in ammonium perchlorate concentration and particle size, and in degree of plasticization. In addition, lead chromate and copper chromite (20) were incorporated in two formulations (RH-P-403 and -404, respectively). Except for variations in plasticizer content (RH-P-402), all compositions maintained the same binder composition; one sample consisted of the binder alone.

As inert-binder propellant, a carboxyl-terminated-polybutadiene (CTPB) composite was chosen for a second series of formulations. Like its NC counterpart the control for this series, RH-C-40cc, did not contain aluminum either. Although its oxidizer content was impractically low from a ballistic-performance standpoint, the resulting formulation gave sufficient latitude within which useful compositional changes could be made. A second CTPB-binder propellant, RH-C-41, with a higher oxidizer loading but with essentially the same binder was used for the study of oxidizer-particle-size effects. This change in reference formulation was dictated by oxidizer settling encountered during cure of original batches of the lower-oxidizer propellant containing large, unimodally distributed oxidizer.

Only a few variations of an NF-binder propellant were made, and those on a single base formulation, since the scope of the investigation did not justify a major effort with this third binder type. Only those formulations were studied for which samples were available from propellant batches prepared for other programs. Nevertheless, the data reported here for NF propellants are probably typical.

Procedure

Calibration of Pressure Transducer and Calibrator - The pressure-transducer—amplifier—calibrator system was calibrated as follows. The output of the transducer was measured several times at each of five pressures between 0 and 20,000 psig. During this procedure the transducer was connected to the calibration unit but the stepping calibrator was set at its lowest value (zero-level output). The transducer outputs (mV) were fitted by a second-order, least-squares regression of the output values on the pressure values. The standard error of estimate of the data when compared with the regression was 7.3 psi. The four step outputs of the calibrator unit (still connected to the transducer but without pressure applied) were then measured. These data were used with the least-squares regression to determine pressures corresponding to the calibrator steps (6,200 psig, 12,500 psig, 19,050 psig, 25,500 psig).

System Check-Out - To check the reproducibility of strand-burner r—P data and the agreement with independent r—P measurements, a series of firings was carried out using strands of RH-P-112cb, a composition well-characterized at low pressures (2)(20). Duplicate firings were made at several pressures to evaluate reproducibility. Strands of two different cross-sectional dimensions ($\frac{1}{4}$-in. - and $\frac{1}{8}$-in. - diam.) were fired. The effects of coating strands with a common restrictor material, Dow-Corning silicone vacuum grease, and the influence of burner working medium, oil or water, were also checked. Low-pressure burning rates were compared with the results of standard, N_2-filled strand-burner firings and of 2-in. -diam. -rocket-motor firings.

As is indicated by the data shown in Fig. 6, the oil-filled 20,000-psig strand burner gave reproducible results, insensitive to the configuration changes tested. Similar checks of reproducibility were also carried out in the course of later, routine firings and involved, for the most part, variations in strand size, pressurizing medium, and strand restriction. In addition, batch-to-batch r—P variations were checked with one of the test propellants.

Sample Preparation - With the exception of the NF-binder samples, all of the strands for which r—P data were measured were cut from single blocks cast from 1000-gm propellant batches. Before testing, small samples were cut from several locations on each block and densities were determined to assure that each block was of uniform composition and had a density near theoretical. Each block was cut into $\frac{1}{4}$-in.-thick, 3-in. × 5-in. slabs, and from these, square-cross-section strands of $\frac{1}{8}$-in. or, in some cases, of $\frac{1}{4}$-inch thickness and $3\frac{5}{8}$ inches long were trimmed. The corners of each strand were further trimmed so that each strand had an approximately octagonal cross-section. The strands were then drilled (No. 78 drill) for the insertion of two fuse wires,* one located about $\frac{5}{16}$ inch from the bottom end of the strand and the other at about the same distance from the top.

The strand was then usually restricted and taped to a $\frac{3}{32}$-in.-diam. wooden swab stick which, in turn, was inserted into the clamp block of the strand-burner firing head. The ends of each fuse wire were spot-soldered to appropriate firing-head electrodes and the small loop of tungsten igniter wire (attached to the firing-head igniter electrodes) was put in intimate contact with the outside edges of the top end of the strand. The sample was then ready for firing.

---

*$\frac{1}{4}$-ampere, "Buss" fuse wire, Bussman Manufacturing Company, St. Louis, Missouri.

NF-propellant samples were prepared in the same manner except for having been cut from ¼-in. × 6-in. × 6-in. slabs from sheet molds.

Firing Procedure - Normal firings involved (1) partially filling the strand-burner can with a light hydrocarbon oil, (2) inserting and tightening the firing head (with strand), (3) pre-pressurizing the burner to 1000 to 2000 psig using bottled nitrogen, and (4) oil-displacement pumping of this nitrogen to the desired test pressure. Calibration steps were recorded on the pressure-transducer recorder channel both before pressurization and after venting the combustion products. The pressure recorder was started before ignition and, in all tests, it was run at a nominal chart speed of 100 mm/sec. Ignition was obtained by manually closing a switch in the ignition circuit. This provided about 14 V a.c. to a B & S No. 20 tungsten igniter wire via an autotransformer. This combination of wire size and applied voltage functioned well and did not necessitate replacement of the igniter wire at each firing. The ignition current was interrupted automatically upon burn-through of the first fuse wire by the relay which started the timer clock.

After the strand burned out, as indicated by a peak pressure on the pressure record, the burner was vented by allowing its internal pressure to force the oil and combustion products within it into the dump can. The firing head was then removed, cleaned with solvent, inspected for damage, corrosion, etc., before being fitted with a new propellant sample.

A typical firing record is shown in Fig. 7.

Results

Most of the experimental results of this study are in the form of regression-rate—vs.—pressure data for plastisol-nitrocellulose and carboxyl-terminated-polybutadiene composite propellants; these are discussed in detail. The results with NF propellants were so meagre that the generalizations which follow cannot be extended to this type.

Control Propellants - Log r—log P plots for the reference propellants are found in Figs. 8 and 9. The consistency of the data despite changes in batch, strand size, and restriction is a favorable indication of the precision of the technique and the creditability of the results.

Oxidizer-Particle-Size Effects - Characteristic of the formulations tested extensively in this study was the tendency of regression rates to become appreciably less dependent on ammonium perchlorate particle size at high pressures. This tendency was particularly pronounced in the inert-binder propellants (Fig. 10), but the range of burning rates between coarse- and fine-oxidizer propellants also decreased with pressure for plastisol-nitrocellulose propellant (Fig. 11). In neither type did the convergence of log r—log P plots for different oxidizer sizes continue beyond 6000 to 10,000 psig. Instead, for both binder types, the plots were approximately parallel and linear in log—log coordinates at high pressures. The linearity and decreased AP-particle-size dependence were exhibited above 6000 psig for the NC propellants tested and above 10,000 psig for the CTPB propellants.

At pressures between 2000 and 8000 psig, below the region of nearly constant pressure index, each propellant type exhibited a transition regime. In this regime, the pressure index either increased monotonically (NC propellant), or increased and then decreased again to its high-pressure value (CTPB). Propellants containing larger oxidizer

particles generally showed higher indexes in the transition regime and this led to a trend toward convergence of the log r—log P plots for different particle sizes.

The nearly constant high-pressure slopes of the plots for the various propellants depended on the binder system involved. The NC propellants showed a slope of 1.0 to 1.3 above 6000 to 8000 psig; the CTPB propellants, a slope of nearly 1.0 above 10,000 psig. The NF system showed a slope of 0.75 to 0.80 above 4000 to 5000 psig (Fig. 12).

With the two formulations in which three oxidizer sizes were tested (RH-P-181 and RH-C-41), an irregularity appeared in the high-pressure data. In the high-pressure regime of nearly constant pressure index, the data for 55μ-wt.-median-diam. AP in NC binder showed a slope of 1.3, about equal to that with coarse oxidizer (175μ), instead of a lower slope as would have been indicated by the value of 1.0 for the finest oxidizer (13μ) (Fig. 11). (Complete particle size distributions are given in Fig. 13.) A hint of similar behavior was found with the CTPB propellant, although the data were too limited to be conclusive (Fig. 10).

Oxidizer-Concentration Effects - Oxidizer-weight-fraction effects were studied only with the NC (Fig. 14) and CTPB propellants (Fig. 15). With both types, the r—P trends as oxidizer concentration was reduced were qualitatively similar to those noted by increasing AP particle size. There was less effect of oxidizer level on regression rate at high pressures than at low. Again, the trend toward a smaller range of regression rates at higher pressures was more pronounced with CTPB propellant than with the NC type.

Decreasing the oxidizer concentration in the CTPB propellant displayed a striking effect on regression rates in the 2000-to-10,000-psig transition regime (Fig. 15). With 60% AP this binder showed extraordinary high pressure indexes between 5000 and 10,000 psig. This low-oxidizer propellant also exhibited a low-pressure deflagration limit between 2500 and 3000 psig; $\frac{1}{8}$-in. strands spontaneously extinguished either shortly after ignition or after only an inch or so of burning. Though this deflagration limit may bear on the high values of the pressure index observed with this propellant, this aspect was not investigated further. One strand was, however, burned under water and gave essentially the same regression rate as was observed under oil.

Aluminum-Concentration Effects - Aluminum-weight-fraction effects on r—P data were examined only with the NC and CTPB propellants. The qualitative behavior of the two binder systems was quite different.

The presence of 15% aluminum powder in the NC propellant yielded a 17% higher regression rate in the low-pressure regime (<3000 psig), but the log r—log P plots were nearly parallel and linear (Fig. 16). With non-aluminized propellant, the pressure index began to increase at a slightly lower pressure and rose faster than with the aluminized form until the two regression rates were equal at about 7500 psig. Slightly higher rates for the non-aluminized propellant were observed above this pressure. Both propellants exhibited nearly linear log r—log P plots at the high end of the pressure range tested, but the slope of the non-aluminized propellant appeared to be slightly higher than that for the propellant with 15% aluminum (1.25 and 1.20, respectively).

In CTPB propellant, 9.1% aluminum powder affected only the transition-regime burning rates, reducing regression rates some 10% between 2000 psig and 12,000 psig (Fig. 17). No conclusive evidence of different regression rates for the aluminized and non-aluminized CTPB propellants was observed at 2000 psig nor above 12,000 psig.

Catalyst Effects - Both NC and CTPB propellants tested showed that catalytic agents promoting burning rates at low pressures lose their efficacy at high pressures. This loss appeared to begin with the onset of the transition regime. The catalytic effects of $PbCrO_4$ with the NC propellant (Fig. 18) and of both ferrocene and copper chromite with the CTPB propellant (Fig. 19) essentially vanished at pressures above 10,000 psig.

Contrary to a previous report (20), copper chromite did not enhance NC propellant regression rate at 2000 psig; it did yield an 8% higher rate within the transition regime, only to lose its effect again above 10,000 psig. The apparent inactivity of copper chromite at low pressure in NC propellant should be checked further.

Effects of Plasticization on Nitrocellulose Propellants - The influence of plasticizer content (plasticizer weight fraction/double-base-powder weight fraction) on the regression rates of NC propellant began to vanish with the onset of transition and was essentially non-existent above 10,000 psig (Fig. 20).

Temperature Effects - The effects of elevated conditioning temperature (+140° F) on r—P data for the NC propellant began to disappear in the transition regime and were negligible above 10,000 psig (Fig. 21). No low-temperature firings of this propellant were made.

CTPB propellant containing 75% AP yielded slightly higher regression rates throughout the whole pressure range tested at 140° F. No irregularity was observed except for a slightly decreased effect within the transition regime (Fig. 22). Low-temperature (-15° F) conditioning of 80%-AP formulations showed similar regularity of effect, with slightly lower regression rates for both 13μ and 175μ particle sizes (Fig. 23).

Transition in Plastisol-Nitrocellulose Binder - Strands consisting of NC binder alone exhibited transition at low pressure (about 2000 psig) (Fig. 24). Time limitations did not allow full characterization of the low-pressure region. The two data points taken (at 2000 and 3000 psig) definitely indicated, however, that the binder material, unlike straight cast or extruded double-base propellants (18), did exhibit an increasing pressure index at elevated pressures. The log r—log P data for the plastisol-nitrocellulose binder lay in a straight line between 8000 psig and 20,000 psig to give a pressure index of about 1.06.

Restrictor Effects - In the course of these experiments several aspects relating to the strand-burning technique itself were observed, especially with regard to strand restriction. The use of liquids such as oil or water as strand-burning media, was attractive as has been pointed out. At pressures below 12,000 psig, no additional restriction was found to be necessary with $\frac{1}{8}$-in. or $\frac{1}{4}$-in. strands. At higher pressures, however, treatment of the strand sides was found to be required with one batch of RH-P-181cb control propellant, with RH-C-41, high-oxidizer, inert-binder propellant, and with the fine-oxidizer NF propellant (RH-SB-103ci-1079).

Dow-Corning silicone high-vacuum grease restrictor gave consistent data with the two plastisol propellants, apparently having no effect on measured regression rates (Figs. 6 and 8). However, this vacuum grease, as well as General Electric's RTV-108, a low-temperature-curing silicone rubber, gave increased regression rates with the inert-binder formulations (Fig. 25).

To reduce or eliminate the low-pressure, restrictor-induced burning-rate enhancement, both uncured Pittsburgh Plate Glass Company's Bondmaster M 666 epoxy adhesive (Part B) and the inert binder alone were tried as restrictors. Only the latter gave encouraging results, but even it was not successful with the high-oxidizer-content, small-particle-size, inert-binder propellant, RH-C-41ce, at 20,000 psig. The binder material did, however, appear to be suitable with RH-C-41cb, and the data reported for this propellant (Fig. 10) are from strands coated with fuel binder.

Water-leaching of the propellants for which the binder material was not effective at high pressure (RH-C-41ce and cc) yielded results consistent with those found for unrestricted strands of the same propellants at lower pressures (Fig. 26).

DIAGNOSTIC EXPERIMENTS REGARDING TRANSITION

Photographic Studies

Before more complicated analytical techniques were attempted, such as product-gas sampling, high-pressure calorimetry, etc., the feasibility of visual observation of deflagration at high pressures was explored. Since the coarse-oxidizer, inert-binder propellant RH-C-41cc, for example, had shown a rather abrupt transition to high index at about 4000 psig, such a propellant might be expected to show visible changes in flame zone, burning-surface structure, or some other physical feature of the deflagration process.

An existing optical strand burner design — the so-called micro window bomb — successfully used for other photographic and spectroscopic studies at these Laboratories at pressures up to 6000 psi was employed (22)(23).

The micro window bomb was attached to the pressurization system for the 20,000-psig strand burner through an accumulator tank of approximately 3 ℓ volume. Nitrogen was charged into the accumulator from 2000-psig gas bottles and was oil-displacement-pumped to 8000 psig; then part of it was bled into the micro window bomb. After firing of the normal propellant sample ($\frac{1}{16}$ inch thick × $\frac{1}{4}$ inch wide × $\frac{5}{8}$ inch long), the combustion products were vented to a dump can. The pressurization and venting systems for the micro window bomb are shown schematically in Fig. 27.

The photographic apparatus and arrangement for these high-pressure firings were the same as for those reported earlier for micro-window-bomb photographs (23), except that all photographs were taken at 0.8 × magnification and a 1000-watt projector was used for back lighting.

In an effort to discover gross physical effects of the transition phenomenon, firings of the control plastisol-nitrocellulose propellant, RH-P-181cb-101, were made at 3000 and 6000 psig, and firings of the coarse-oxidizer, low-oxidizer-content CTPB propellant, RH-C-40cc-101, were made at 2000, 3000, 5000 and 7000 psig. In some cases, duplicate firings were made to check qualitative observations and to provide records duplicating firings for which exposure, camera operation, etc., were not satisfactory. Twelve firings were made in all.

The results of the photographic experiments using the micro window bomb at high pressures were in the form of a series of 16-mm color motion-picture films taken at 2000 to 4000 frames/sec.

No marked differences among the various firings of either propellant were apparent from the photographs. Firings at different combustion pressures displayed some change in appearance of the propellant flame zone but not more than was anticipated to result from pressure variation only. There was no evidence of ejection of solid-phase material from the surface, except for some large pieces of what seemed to be carbonaceous material originating at the edges of the burning CTPB propellant.

Thermal-Stress-Induced Fracture of Oxidizer Crystals

To investigate further one of the theories of transition in pure pressed strands of ammonium perchlorate (12), a simple experiment was carried out on large AP particles. The theory postulates the occurrence of fracture of AP crystals under thermal stresses resulting from passage of solid AP through the thermal wave in the course of combustion. Owing to concomitant polymorphic transformation, sublimation of, and decomposition of AP, this fracture mechanism is

probably not independent of other processes. Nonetheless, attempts were made to determine whether AP particles could be fractured by the stresses resulting solely from thermal expansion in a varying-temperature environment.

Procedure - Large particles of commercial AP,* of spheroidal shape and having a weight-median diameter of 350μ, were conditioned in a liquid-nitrogen bath. A photomicrograph of some of these crystals is shown in Fig. 28. As a control sample, a portion of the crystals was left in the bath to warm up slowly to room temperature as the nitrogen boiled away. The remainder was dropped quickly, still in liquid nitrogen, into a vessel of toluene at room temperature. Being less dense than toluene, the liquid nitrogen remained on the toluene surface and quickly boiled away. The AP particles sank into the toluene phase and in so doing presumably underwent an extreme thermal shock. Some of the control sample (after having warmed up to room temperature following evaporation of the liquid nitrogen) was also dropped into room-temperature toluene. These three samples (two controls) were then viewed microscopically and photomicrographed at about 12 X magnification.

Results - No change in either of the control samples could be detected when compared with samples of the original AP crystals. By contrast, numerous very fine particles were observed in the thermally shocked sample. A sample of these fine particles is shown in Fig. 29, reproduced at the same magnification as that of Fig. 28. Fig. 31 shows a higher-magnification (approx. 40 X) photograph of the remaining large particles (from which the sample of fine

---

*"Trona"-brand, American Potash and Chemical Corporation, New York, New York, coated with 1% tricalcium phosphate.

particles had been separated), for comparison with Fig. 30, a similar photograph of the control sample. Considerable cleavage (nearly planar) of the large crystals is apparent.

Conclusions - Thermal shock leading to stress can readily produce fracture of AP crystals. Thus, AP particles in solid composite propellants may break up under the action of suitable deflagration-wave temperature gradients. This phenomenon may occur either with or without polymorphic solid-phase transition, sublimation, and thermal decomposition. Therefore, as has been suggested (5), it is a possible contribution to the observed transition of AP deflagration to indexes at high pressures.

A MECHANISTIC MODEL OF HIGH-PRESSURE SOLID-PROPELLANT COMBUSTION

This section presents a qualitative model of the mechanism of regression-rate transition in ammonium perchlorate-containing propellants. The model takes cognizance of and is prompted by the experimental results of the foregoing program. It is not a detailed model nor, in view of its phenomenological complexity, is it readily treated quantitatively. Further development depends on experimental results to be obtained in the future.

Several qualitative empirical aspects of high-pressure solid-propellant combustion should be borne in mind relating to a mechanistic discussion of the transition phenomenon. The occurrence of a region of increasing pressure index at intermediate pressures (2000 to 10,000 psig) appears to be common to all AP-oxidized propellants. The maximum slope exhibited by log r—log P plots of strand-burning data for these propellants depends on the nature of the propellant matrix.

Similarly,the shapes of log r—log P plots in the pressure region of this transition depend on matrix or binder type. These shapes differ substantially among types of reactive binders. In addition to these dependencies, the slopes and shapes of plots for representative propellants show a strong dependence on oxidizer particle size and concentration. These observations must be accounted for in any model of the transition process in AP-containing propellants.

From the data obtained here and from other sources, two distinct regimes of combustion may be defined: Combustion at low pressures (below 2000 psig) and combustion at high pressures (above 10,000 psig).

At low pressures, typical composite propellant formulations undergo (1) binder gasification by pyrolysis or heterogeneous reaction to form gaseous oxidizable species, (2) AP gasification and subsequent gas-phase decomposition, and (3) reactions between gases from the binder and gaseous products of the AP, but not excluding possible heterogeneous catalysis. The burning rate of propellants in this pressure region is presumably dependent on mass diffusion rates and chemical reaction rates, the extent and pressure-dependence of these rates governing the interdependency of the three processes listed above.

At higher pressures, a competing mechanism affects the r—P relations of AP-containing propellants. As the test pressure is increased, the decomposition of AP particles becomes more and more independent of the binder gasification. Decreased mass diffusion rates and, more important, the drastically increased deflagration rate of pure AP in this regime combine to give localized AP decomposition – the oxidizer particles begin to burn at the burning surface as monopropellant particles surrounded by binder which is pyrolyzed independently. Binder pyrolysis occurs primarily under the action of heat feedback from the fuel—oxidizer reaction and is less strongly influenced by heat release during the AP decomposition reactions. The rapidly increasing regression rate of the AP particles, as indicated by the transition of pure AP (v. s.), allows them to burn out quickly, leaving craters or small vermiform holes in the surrounding binder material. The extent of this action depends on the balance between binder regression and oxidizer regression, being more pronounced for inert binders (those containing no oxidizing functions) than for reactive ones and more pronounced for less reactive binders than for more reactive ones. It is also dependent on AP particle size, increasing as particle size s increased.

At pressures above, say, 10,000 psig, localized AP combustion continues to a point where, with any but very reactive binders, the regression of AP particles occurs much faster than that of the binder, leaving behind a thin layer of binder which must react before a succeeding AP particle can be exposed and begin to burn. Thus, the regression rate of this binder layer comes to control the measurable burning rate of the propellant; the nature of burning in this regime is strongly dependent on the binder type and depends only mildly on AP particle size. This slight particle-size dependence arises from the details of the burning surface configuration (geometry) and the fact that there may still be a dependence of the binder regression on AP decomposition (though appreciably less than at lower pressures and lower AP burning rates). This description can be termed "series-burning", owing to its appearance as a successive regression of one AP particle, followed by a layer or region of binder, and then by regression of another particle.

The pressure region where the exponent transition occurs is, of course, the region where the series-burning mechanism gains increasing importance in determining the burning rate.

This model is qualitatively consistent with observed transition phenomena in plastisol-nitrocellulose, inert-binder, and NF propellants. In particular, it can be used as a basis for qualitative exploration of oxidizer-particle size and oxidizer-weight-fraction effects on high-pressure r—P data.

CONCLUSIONS AND RECOMMENDATIONS

On the basis of this investigation, a fuller view of the effects of composition variations on composite propellant transition to high pressure index at high combustion pressures is now available. From the reported r—P data for both an inert-binder and a plastisol-nitrocellulose propellant, it appears that the major compositional influences on burning-rate transition are those resulting from variations in binder type, AP size, and AP concentration.

The incorporation of small percentages of aluminum and several burning rate promoters in both propellant types appears to have no major influence on r—P trends at high pressures. Changes in plastisol-nitrocellulose binder composition are also of small effect. The same observation appears to hold for the influence of conditioning temperature on r—P trends at high pressures. Based on a small amount of data, similar conclusions may be drawn regarding trends in NF propellants, although these conclusions are not yet firmly established.

For propellants of a given binder type, changes in AP content or particle size are the most influential changes observed in the transition regime. Increases in AP concentration or decreases in particle size lead to less abrupt transitions to high pressure index at high pressures. In other words, such changes result either in lower log r—log P slopes at a given high pressure or in a trend toward convergence of such curves at pressures above about 4000 psi (although this convergent trend is not maintained in the face of continued elevation of combustion pressure). In general, all propellant binder types appear to exhibit nearly linear, parallel log r—log P plots for formulations of varying AP particle size and concentration at pressures above 8000 to 10, 000 psig.

Binder type is observed to have a profound influence on the trends of r—P data at high pressures. In general, the more reactive the binder, the less abrupt the change to high pressure index at high combustion pressures. The reactive-binder propellants tested exhibited monotonic trends to an increased, but nearly constant pressure index at higher pressures. There appears to be a correlation between the reactivity of binders of different types and the pressure index ultimately achieved at high pressures by propellants based on these binders. Increasing binder reactivity appears to result in increasing post-transition pressure indexes, although the index varies little from one binder to another.

The trends observed in the compositional influences on transition are consistent with a series-burning model of composite propellant combustion at high pressures. Quantitative verification of the validity of this model would, however, prove difficult. Nonetheless, the characterization of transition made available by the data of this investigation lends appreciable support to a view of the transition regime as a combustion regime intermediate between combustion at low pressures by one mechanism and at high pressures by another. The high-pressure mechanism may be speculated to be a consequence of the transition of pure AP (mechanism still uncertain) and its effect in producing a series-burning situation. In this situation, combustion of individual AP particles which occur very quickly at high pressures must be followed by slower pyrolysis of layers of binder material before ignition of successive AP particles can be accomplished by the gas-phase flame. r—P trends are, therefore, strongly dependent on binder reactivity and the abruptness of transition is greater for inert-binder propellants which pyrolyze considerably more slowly than the fast-burning AP particles. Increasing binder reactivity decreases the tendency of AP particles to burn faster than the surrounding fuel matrix and hence decreases the abruptness of the pressure-index transition.

It is recommended that:

(1) NF propellants be tested further to provide more useful data for comparison with those of the reactive-binder system (plastisol-nitrocellulose) already tested extensively;

(2) an attempt be made to characterize the combustion of NF binder itself, as has already been done with a plastisol-nitrocellulose binder material;

(3) the effects of plasticizer variations in NF binders be investigated as a possible further clue to the influence of binder type on high-pressure r—P relations; and

(4) an unmodified double-base propellant of well-characterized high-pressure regression rate be studied for comparison with other reactive binders and that an AP-modified composition including this binder also be tested.

REFERENCES

1. R. B. Cole, "Combustion of Solid Propellants at High Pressures--A Survey," Rohm & Haas Company, Special Report No. S-71, 39 pp., May 20, 1965 (Confidential).

2. S. E. Anderson, Rohm & Haas Company, private communication, January 1965.

3. J. L. Chaille, "Ballistic Evaluation of High-Burning-Rate NF Propellants," Rohm & Haas Company, Special Report No. S-63, 18 pp., May 13, 1965 (Confidential).

4. O. R. Irvin, W. H. Andersen, R. D. Erickson, "Susceptibility of Solid Composite Propellants to Explosion or Detonation," Aerojet-General Corporation, Final Summary Report 0253-02-12, 50 pp., April 20, 1961 (Confidential).

5. O. R. Irvin, P. K. Salzman, W. H. Andersen, "Deflagration Characteristics of Ammonium Perchlorate at High Pressures," Ninth Symposium (International) on Combustion, Academic Press, New York (1963), pp. 358-365.

6. A. R. Glazkova, "The Effect of Pressure on the Rate of Combustion of Ammonium Perchlorate," Zh. Prikl. Mekhan. i Tekhn. Fiz., 1963, 121-125.

7. M. Summerfield, Princeton University, unpublished data in co-operation with Picatinny Arsenal, January 1962.

8. A. Strasser, "Determination of the Burning Characteristics of Solid Propellants at Pressures up to 50 Kpsi," SPIA Publication X/5 (Bulletin of the Conference on High Nitrogen Content Compounds), pp. 89-97, September 1950 (Confidential).

9. R. W. Walker, J. L. Chaille, C. O. Metzger, "High Pressure Burning Rates of Double-Base and Modified Double-Base Propellants," Bull. 9th Mtg. JANAF Solid Prop. Group, I, 255-264 (1953) (Confidential).

10. D. Flanagan, Thiokol Chemical Corporation (Huntsville), private communications, November, December 1964.

11. J. L. Chaille, Rohm & Haas Company, private communications, October 1964.

12. O. R. Irvin, P. K. Salzman, W. H. Andersen, "Mechanism of the Accelerated Burning of Ammonium Perchlorate at High Pressures," AIAA J., 1, 1178-1179 (1963).

13. R. Anderson, United Technology Center, remarks on heterogeneous chemical reaction combustion mechanism theory at the First ICRPG Meeting on Combustion Instability, November 19, 1964 (Confidential).

14. R. Anderson, United Technology Center, private communication, May 1965.

15. C. Huggett, "Combustion of Solid Propellants," Combustion Processes (Vol. II, Series on High Speed Aerodynamics and Jet Propulsion), Princeton University Press, Princeton (1956), pp. 541-542.

16. M. Barrère, A. Jaumotte, B. F. DeVeubeke, J. Vanderkerchove, Rocket Propulsion, Elsevier, New York (1960), pp. 197-198.

17. C. E. Hermance, "Comparison of Solid Propellant Burning Rates in Strands and Rocket Motors," M. S. E. Thesis, Princeton University, 37 pp. (1961).

18. H. L. Greenwald, C. O. Metzger, E. A. Taylor, "Water as a Medium for Strand Burning at High Pressures," Bull. 8th Mtg. JANAF Solid Prop. Group, II, 409-419 (1952) (Confidential).

19. J. L. Chaille, Rohm & Haas Company, private communication November 1964.

20. William W. Seaton, "Plastisol Handbook," Rohm & Haas Company, Ballistics Section Progress Report No. 114 (internal report), 5 pp. plus Appendices, March 24, 1964 (Confidential).

21. S. E. Anderson and B.L.Thompson, "Ballistic Characteristics of NF Propellants," Rohm & Haas Company, Special Report No. S-85, October 1965 (Confidential)

22. _____, Rohm & Haas Company, Quarterly Progress Report on Interior Ballistics, Report No. P-64-22, pp. 47-50, November 25, 1964 (Confidential)

23. R. H. W. Waesche, "A Spectrographic Technique for the Study of Solid Propellant Combustion," Rohm & Haas Company, Special Report No. S-75, p. 7, July 15, 1965 (Confidential).

PROPELLANT INDEX TO FIGURES

Designation	Figures
RH-C-40cc	22
RH-C-40ce	9, 15, 17, 19
RH-C-41cb	10, 26
RH-C-41cc	10, 23, 26
RH-C-41ce	9, 10, 15, 23, 25, 26
RH-C-42ce	19
RH-C-43ce	19
RH-C-46ce	15
RH-C-49ce	17
RH-P-112cb	6, 16
RH-P-181cb	8, 11, 14, 16, 18, 20, 21, 24
RH-P-181cc	11
RH-P-181ce	11
RH-P-402cb	20
RH-P-403cb	18
RH-P-404cb	18
RH-P-408cb	14
RH-SB-103cd	12
RH-SB-103ci	12

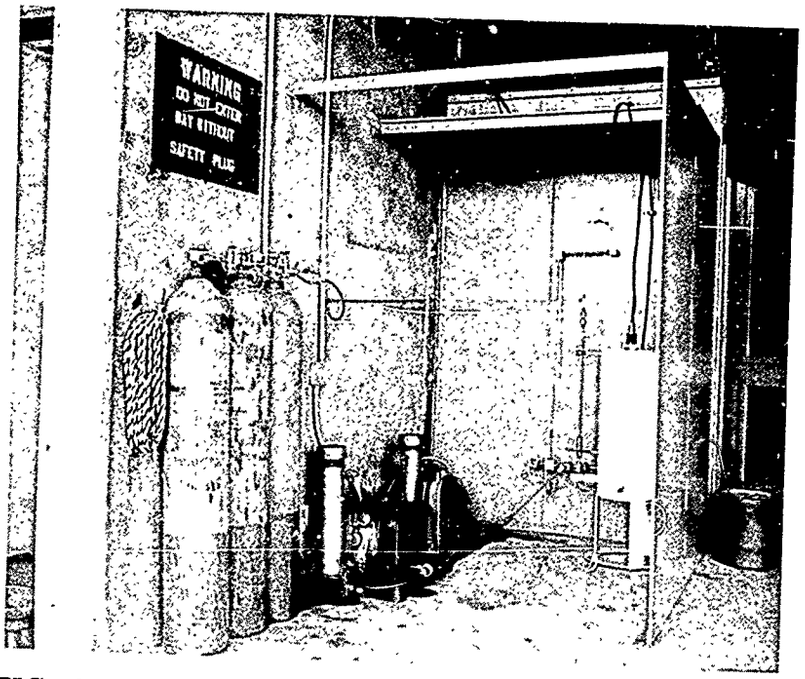

FIG. 1 20,000-psig Strand Burner and Test Cell

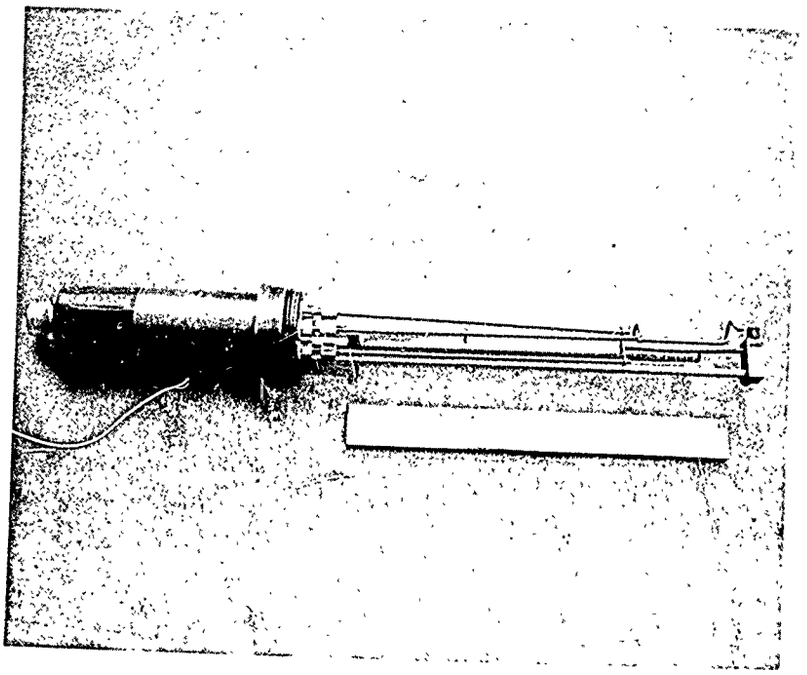

FIG. 2 Firing Head with Propellant Sample in Place

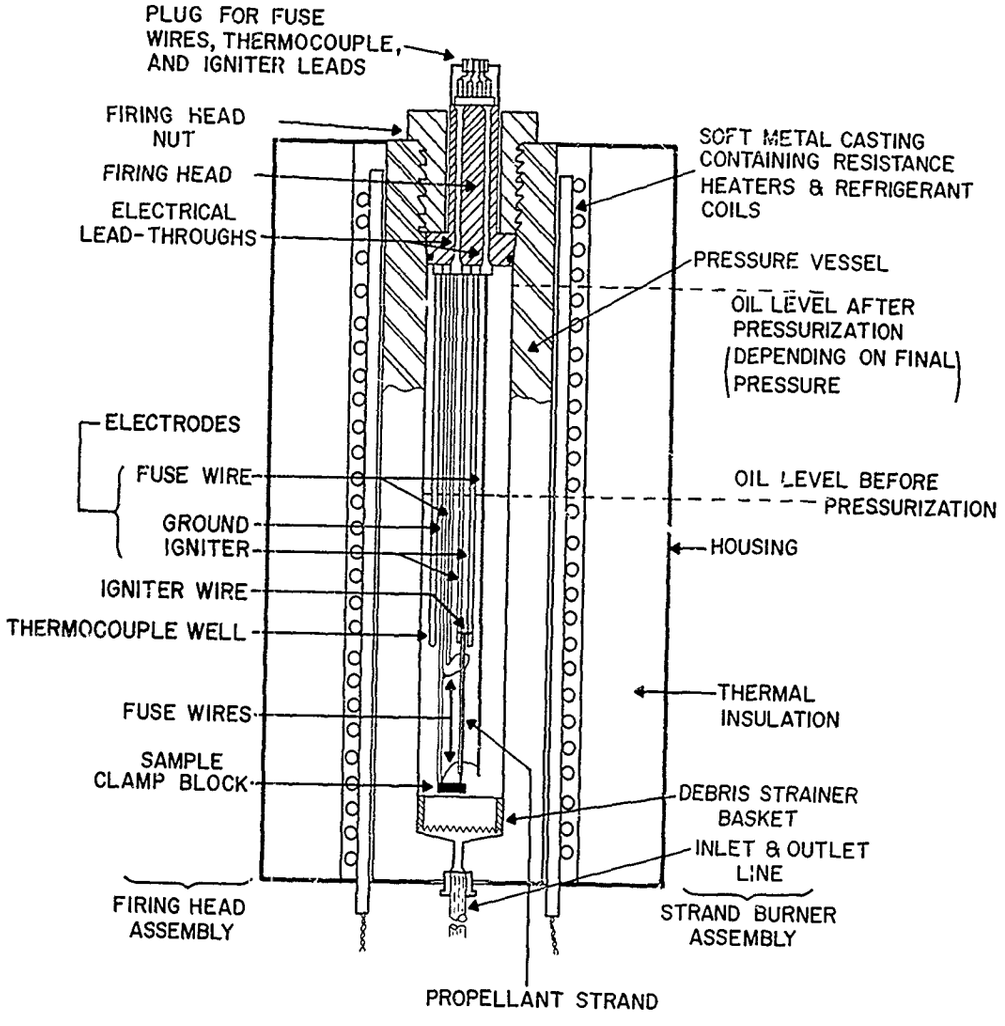

FIG. 3 Sectional View of 20,000-psig-Strand-Burner Assembly

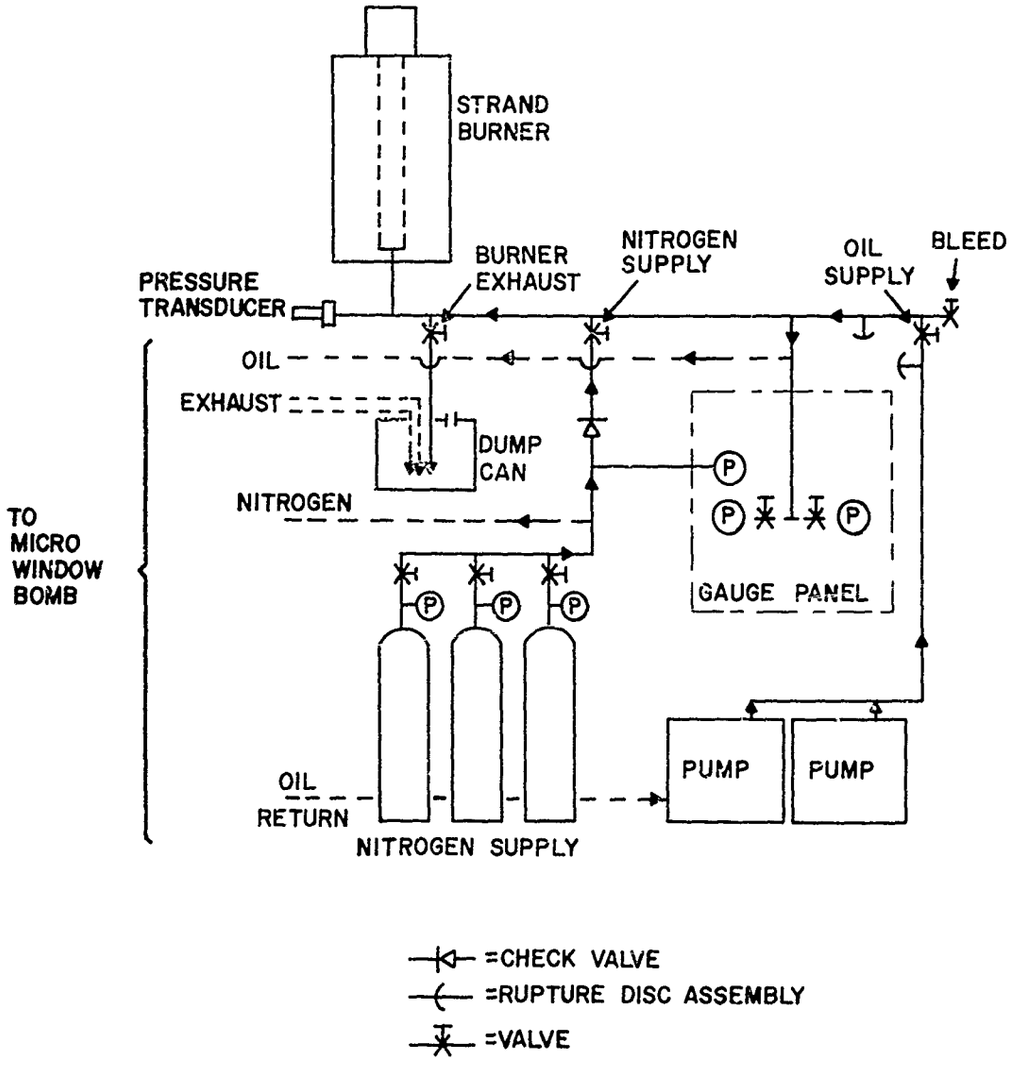

FIG. 4 Schematic Diagram of Strand-Burner Pressurization System

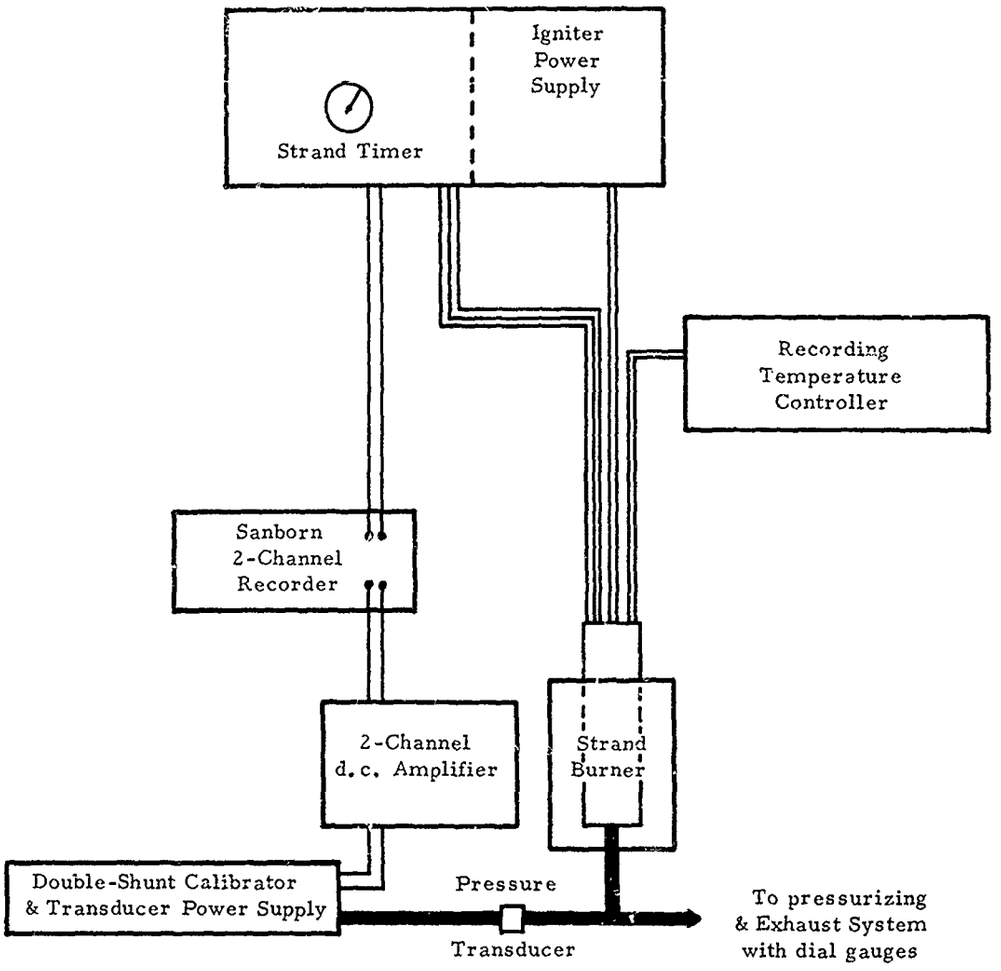

FIG. 5 Schematic Diagram of Strand-Burner Instrumentation

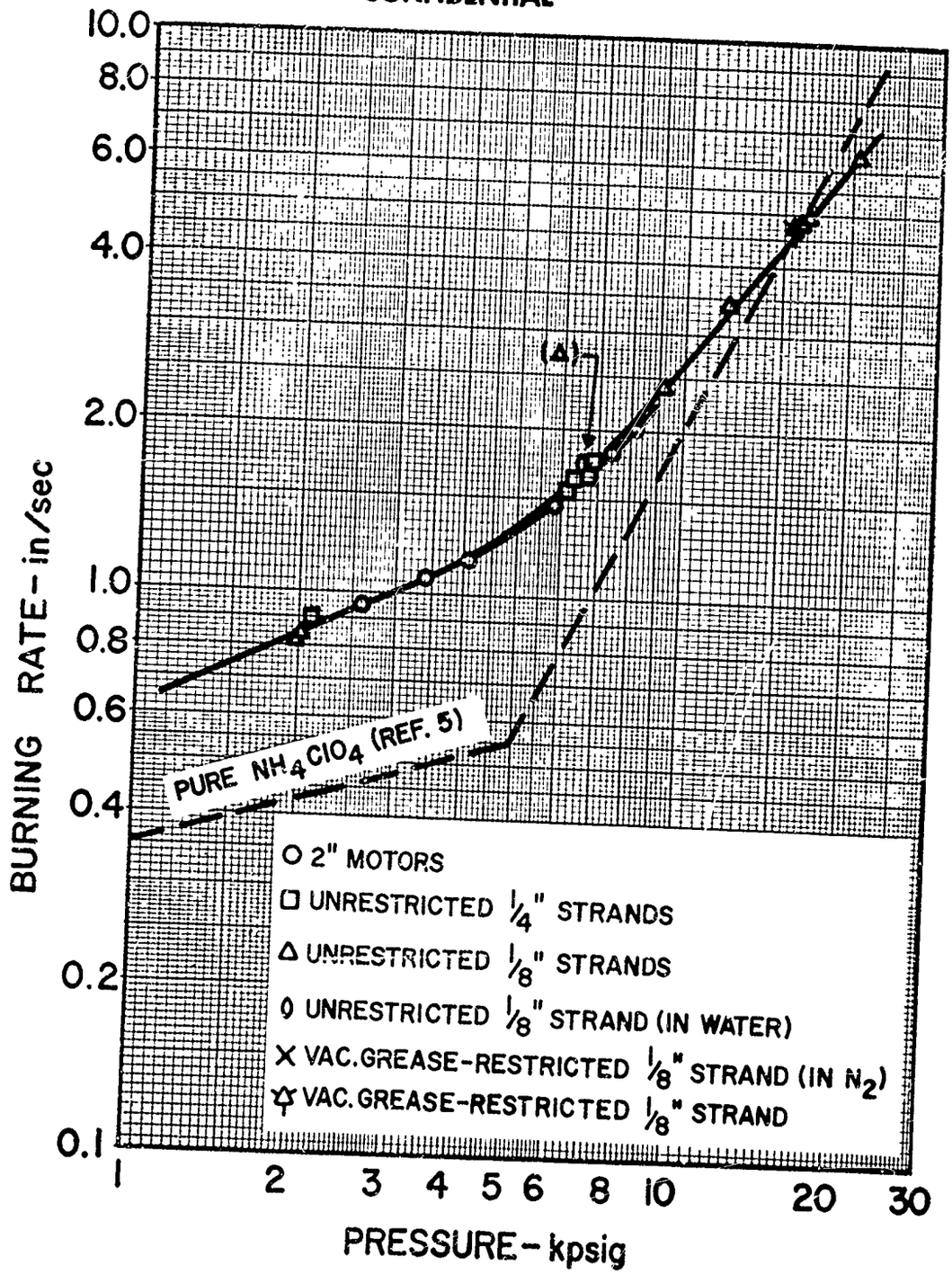

FIG. 6 r—P Data from Strand-Burner Check-Out [RH-P-112cb]

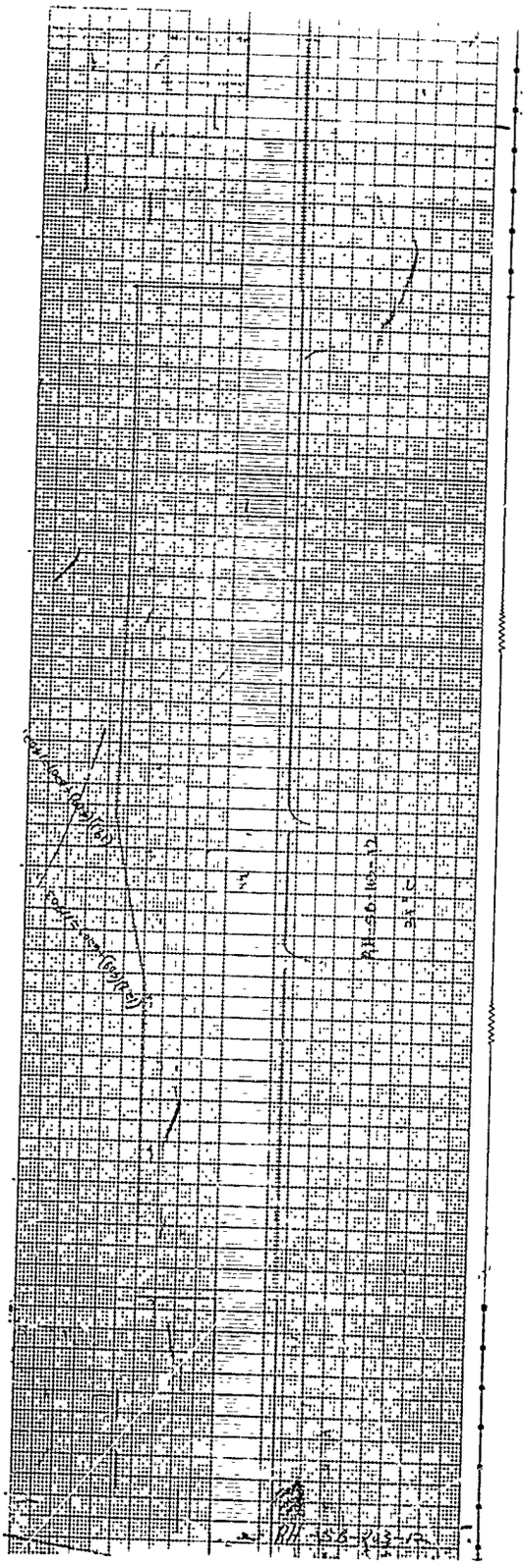

FIG. 7 Typical Strand-Burner Firing Record

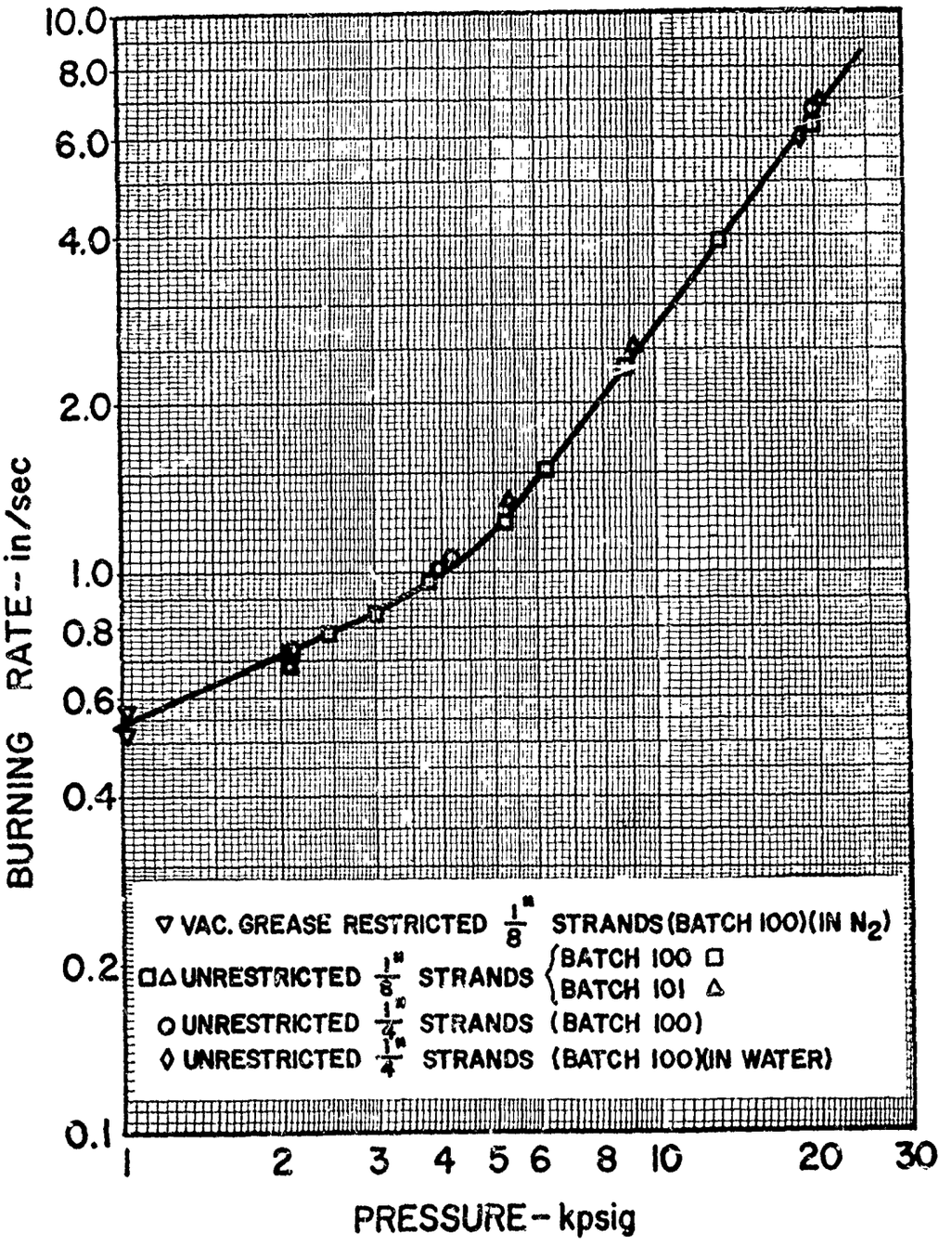

FIG. 8 Burning Rate of Plastisol-Nitrocellulose Control Propellant at High Pressures [RH-P-181cb]

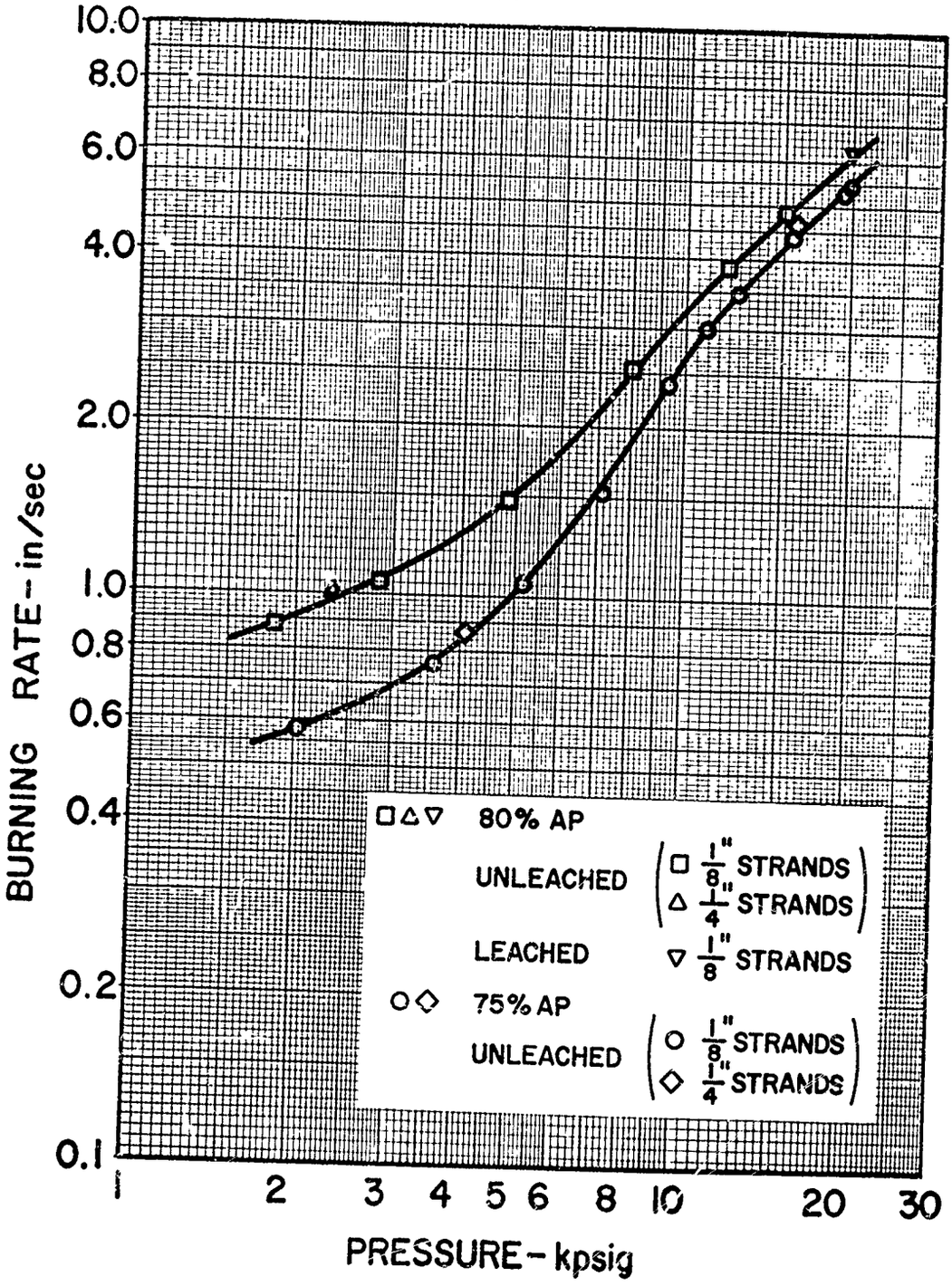

FIG. 9 Burning Rates of Carboxyl-Terminated-Polybutadiene Control Propellants at High Pressures (unrestricted strands) [RH-C-40ce (75% AP) and -41ce (80% AP)]

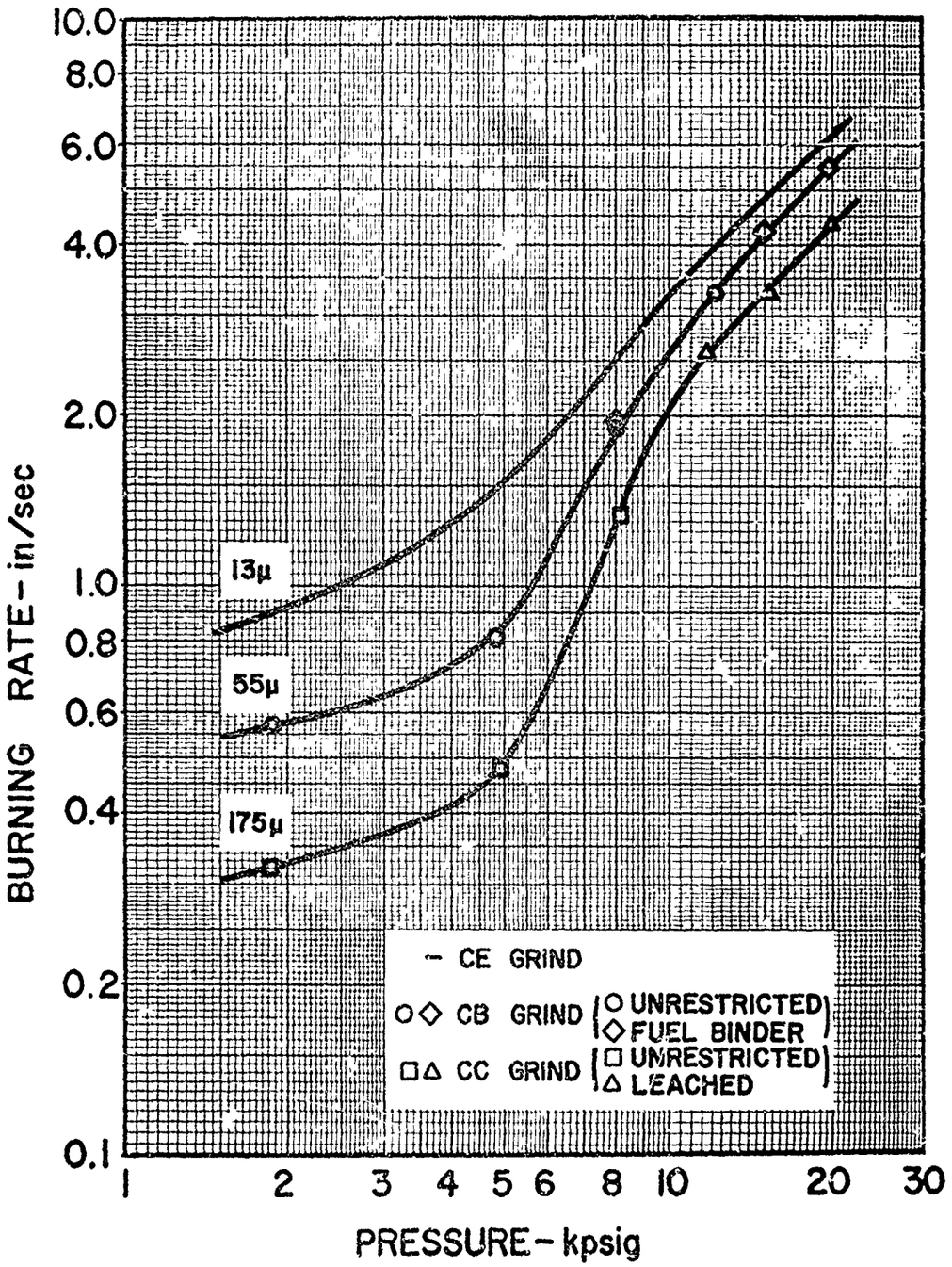

FIG. 10 Oxidizer-Particle-Size Effects on High-Pressure Burning Rates of Ammonium Perchlorate-Containing Inert-Binder Propellant ($\frac{1}{8}$-in. strands)[RH-C-41cb, cc, and ce]

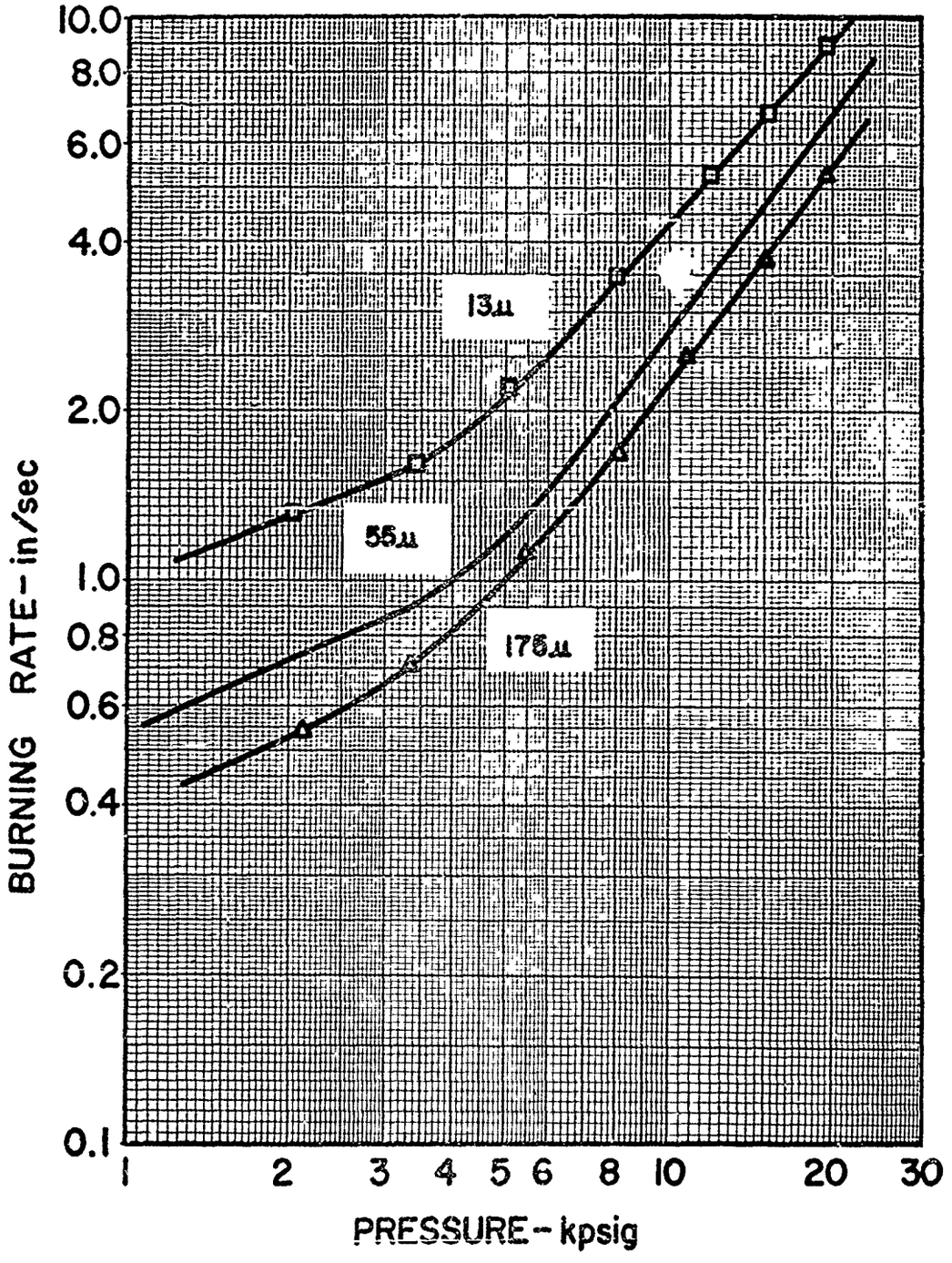

FIG. 11 Oxidizer-Particle-Size Effects on High-Pressure Burning Rates of Ammonium Perchlorate-Containing Plastisol-Nitrocellulose Propellant ($\frac{1}{8}$-in. unrestricted strands) [RH-P-181cb, cc, and ce]

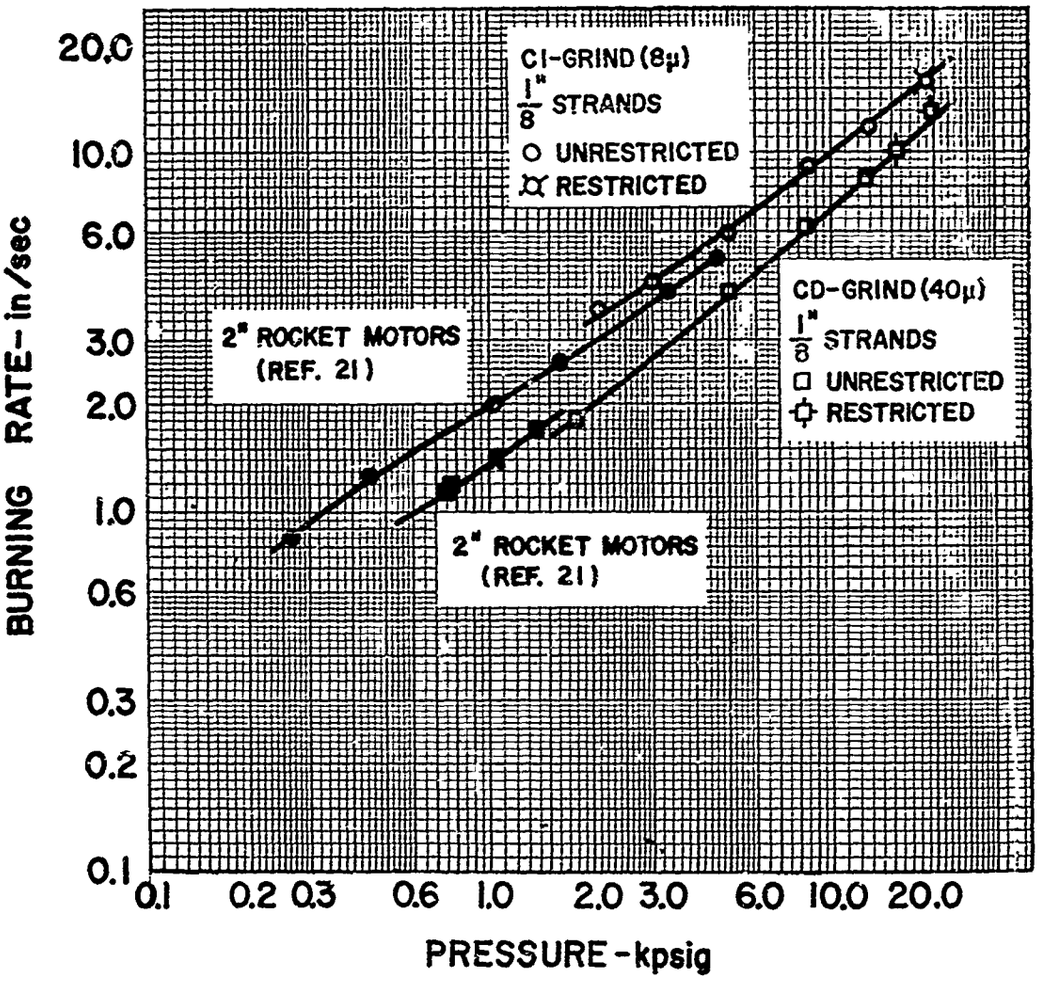

FIG. 12 Comparison of Ammonium Perchlorate-Particle-Size Effects on Burning Rates in Strands and Motors [NF propellants RH-SB-103cd and ci]

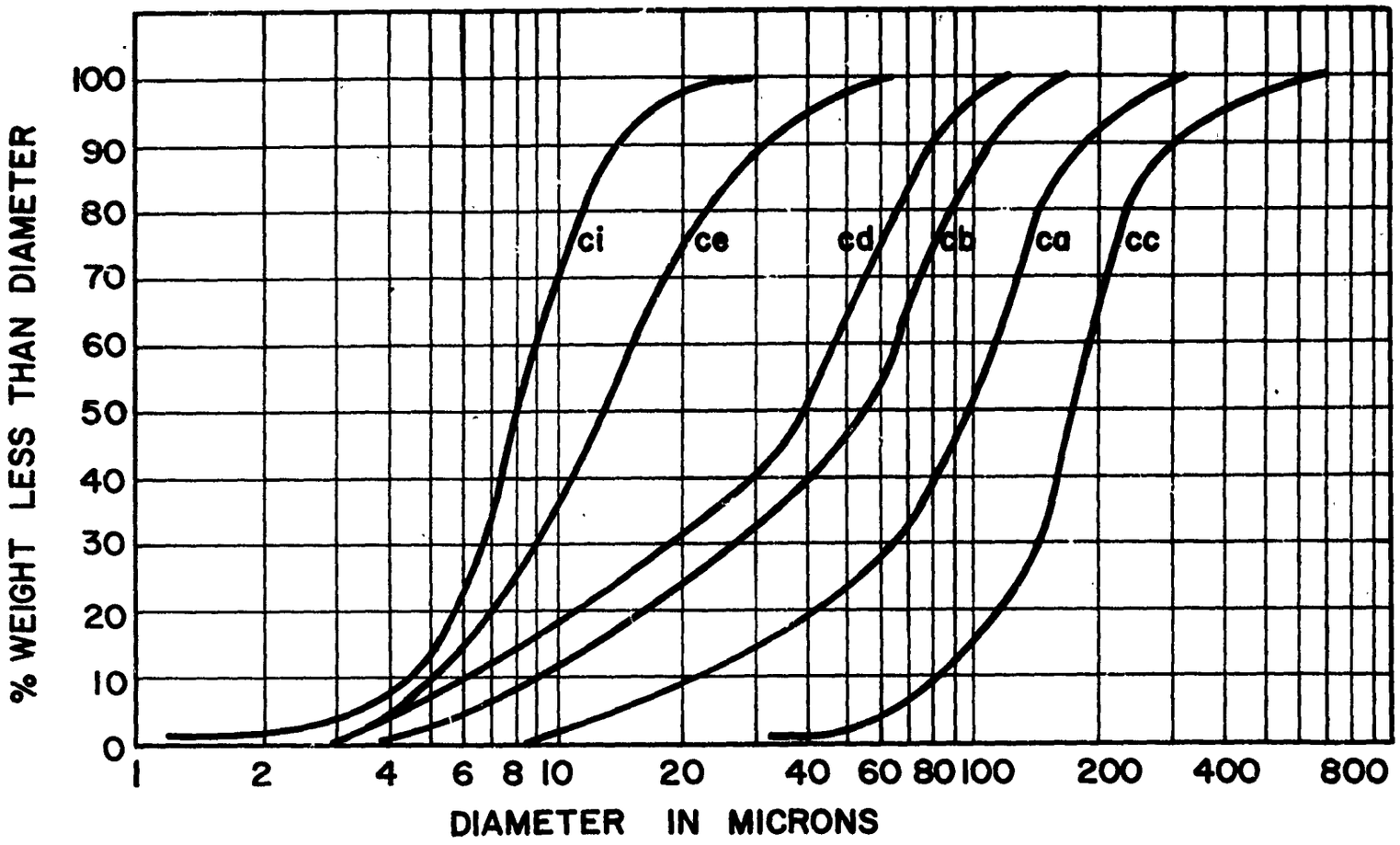

FIG. 13 Nominal Particle-Size Distributions of Ammonium Perchlorate Oxidizer (Micromerograph)

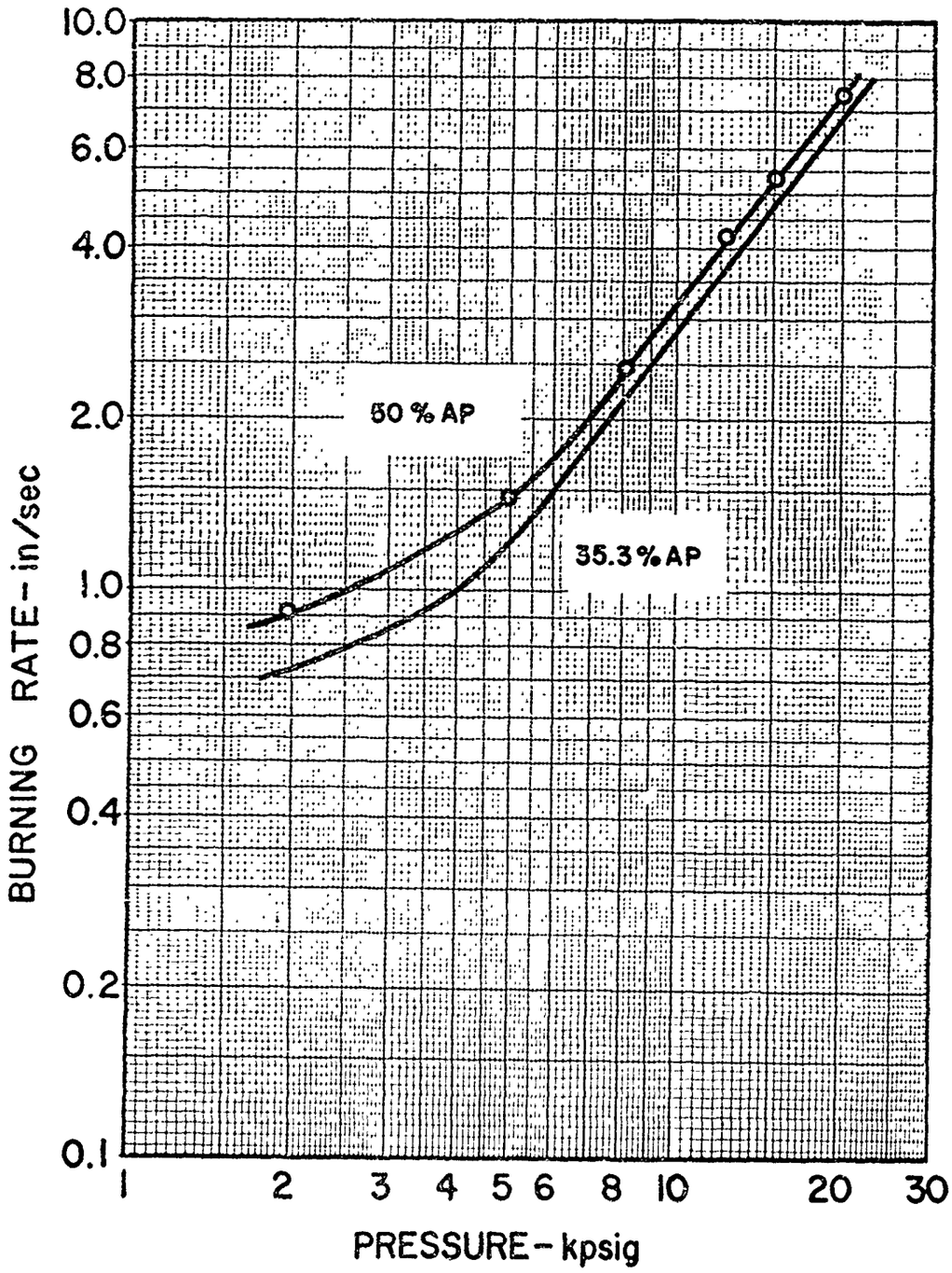

FIG. 14 Oxidizer-Weight-Fraction Effects on High-Pressure Burning Rates of Plastisol-Nitrocellulose Propellants ($\frac{1}{8}$-in. unrestricted strands)[50% AP: RH-P-408cb; 35.3% AP: RH-P-181cb]

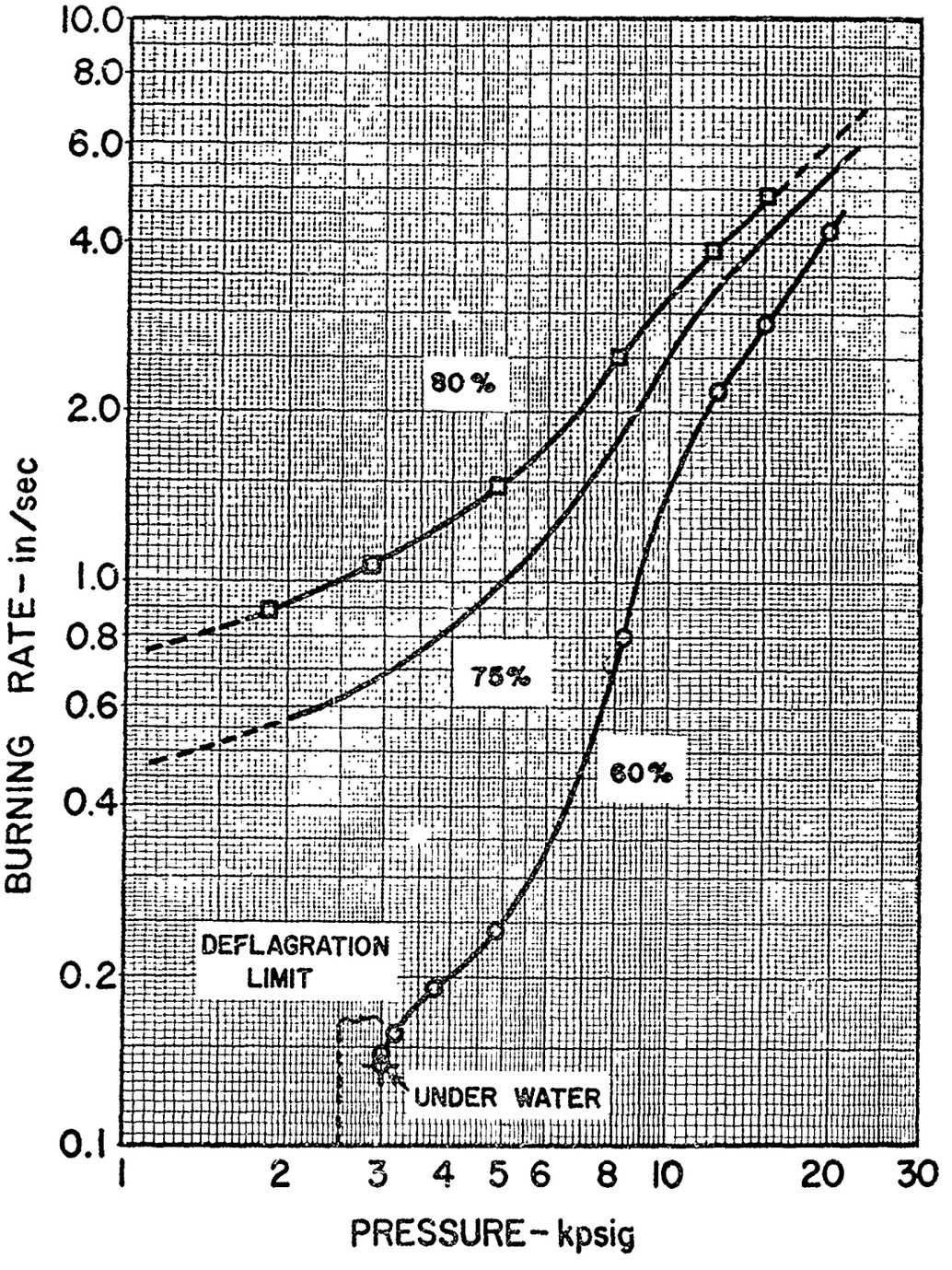

FIG. 15 Oxidizer-Weight-Fraction Effects on High-Pressure Burning Rates of Inert-Binder Propellants ($\frac{1}{8}$-in. unrestricted strands) [80% AP: RH-C-41ce; 75% AP: RH-C-40ce; 60% AP: RH-C-46ce]

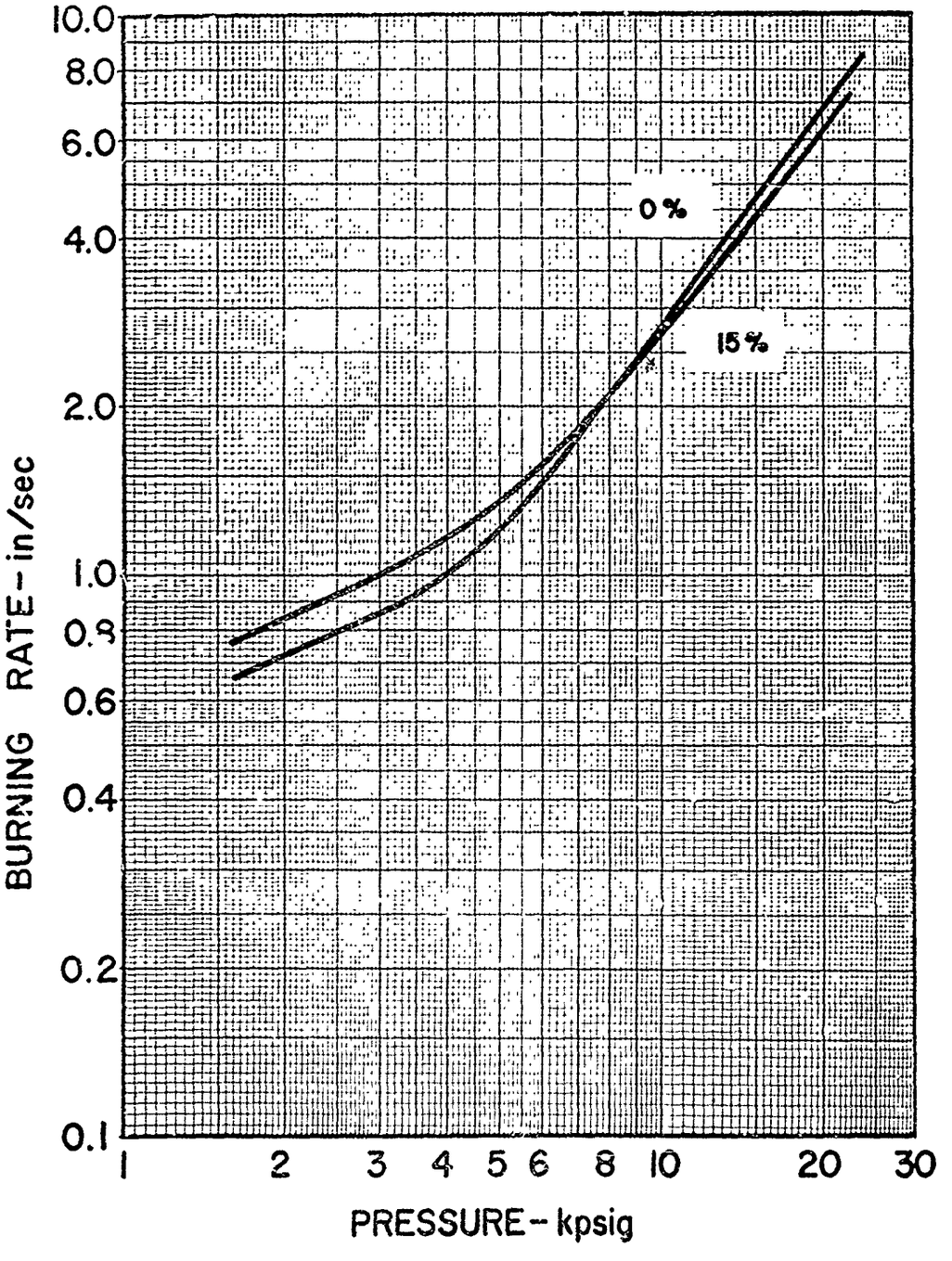

FIG. 16 Effect of Aluminum on High-Pressure Burning Rates of Plastisol-Nitrocellulose Propellants ($\frac{1}{8}$-in. unrestricted strands)[0%: RH-P-181cb; 15%: RH-P-112cb]

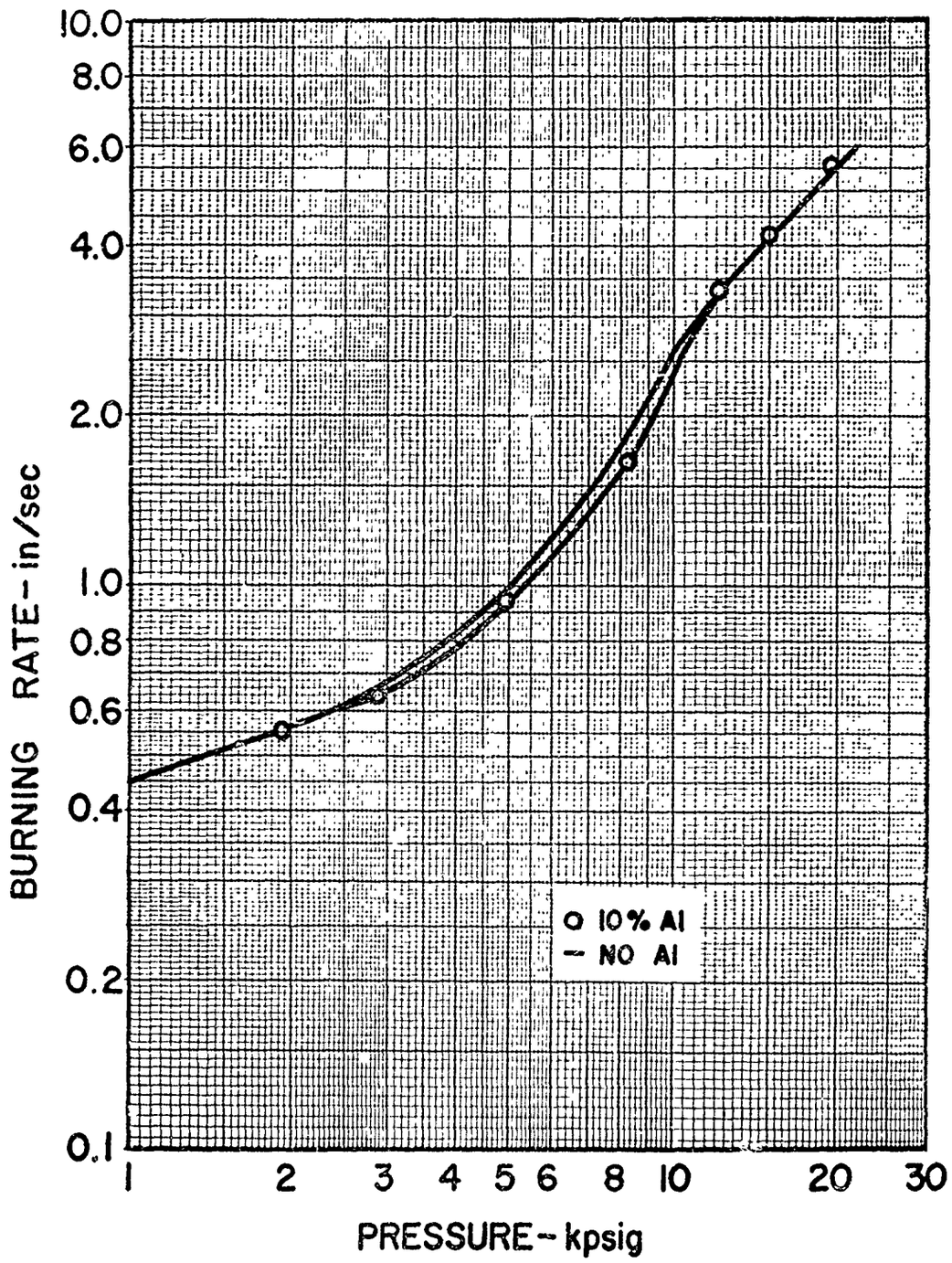

FIG. 17 Effect of Aluminum on High-Pressure Burning Rates of Inert-Binder Propellants ($\frac{1}{8}$-in. unrestricted strands) [0%: RH-C-40ce; 10%: RH-C-49ce]

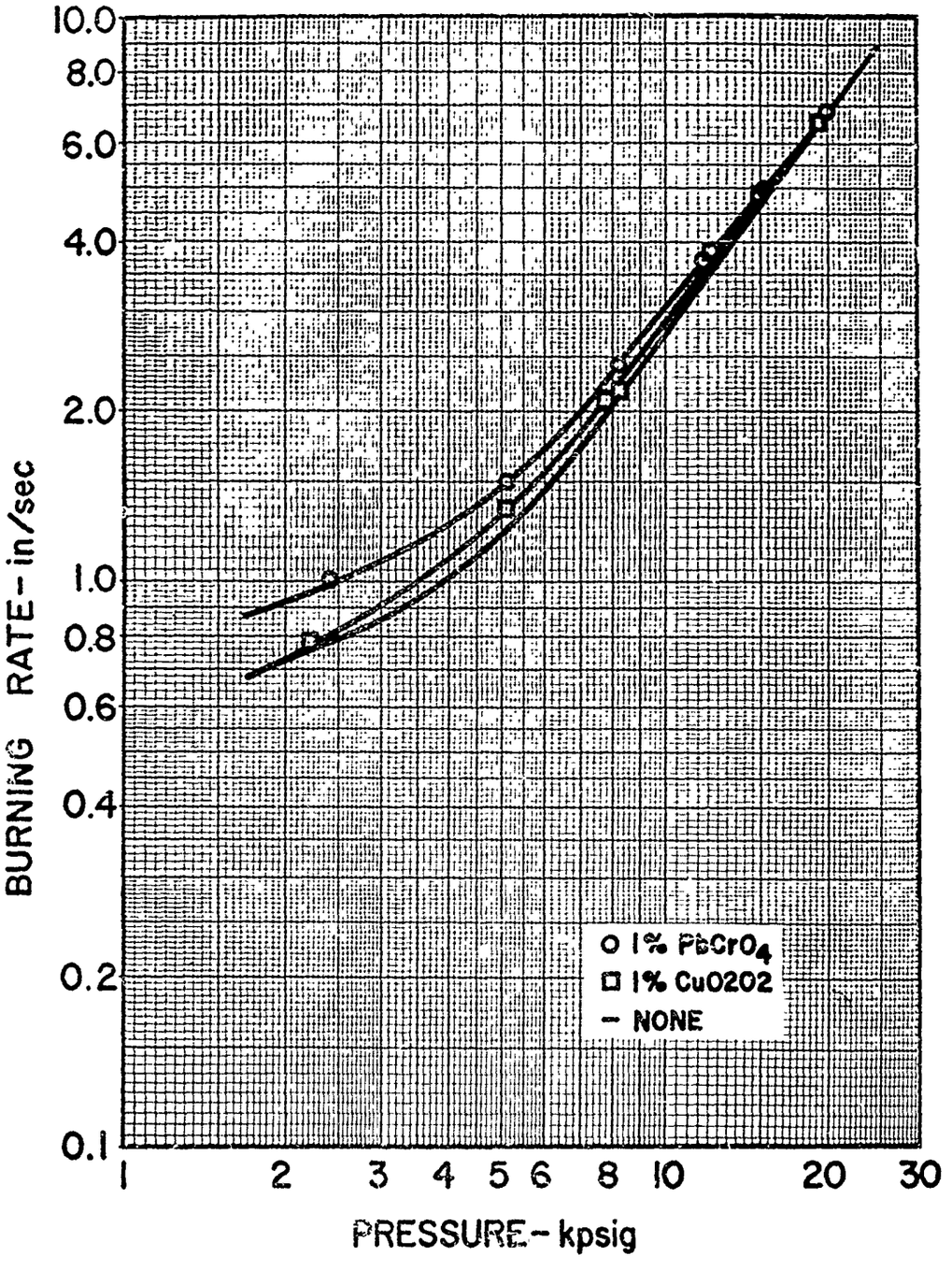

FIG. 18 Effect of Catalysts on High-Pressure Burning Rates of Plastisol-Nitrocellulose Propellants ($\frac{1}{8}$-in. unrestricted strands)[1% $PbCrO_4$: RH-P-403cb; 1% Cu0202: RH-P-404cb; none: RH-P-181cb]

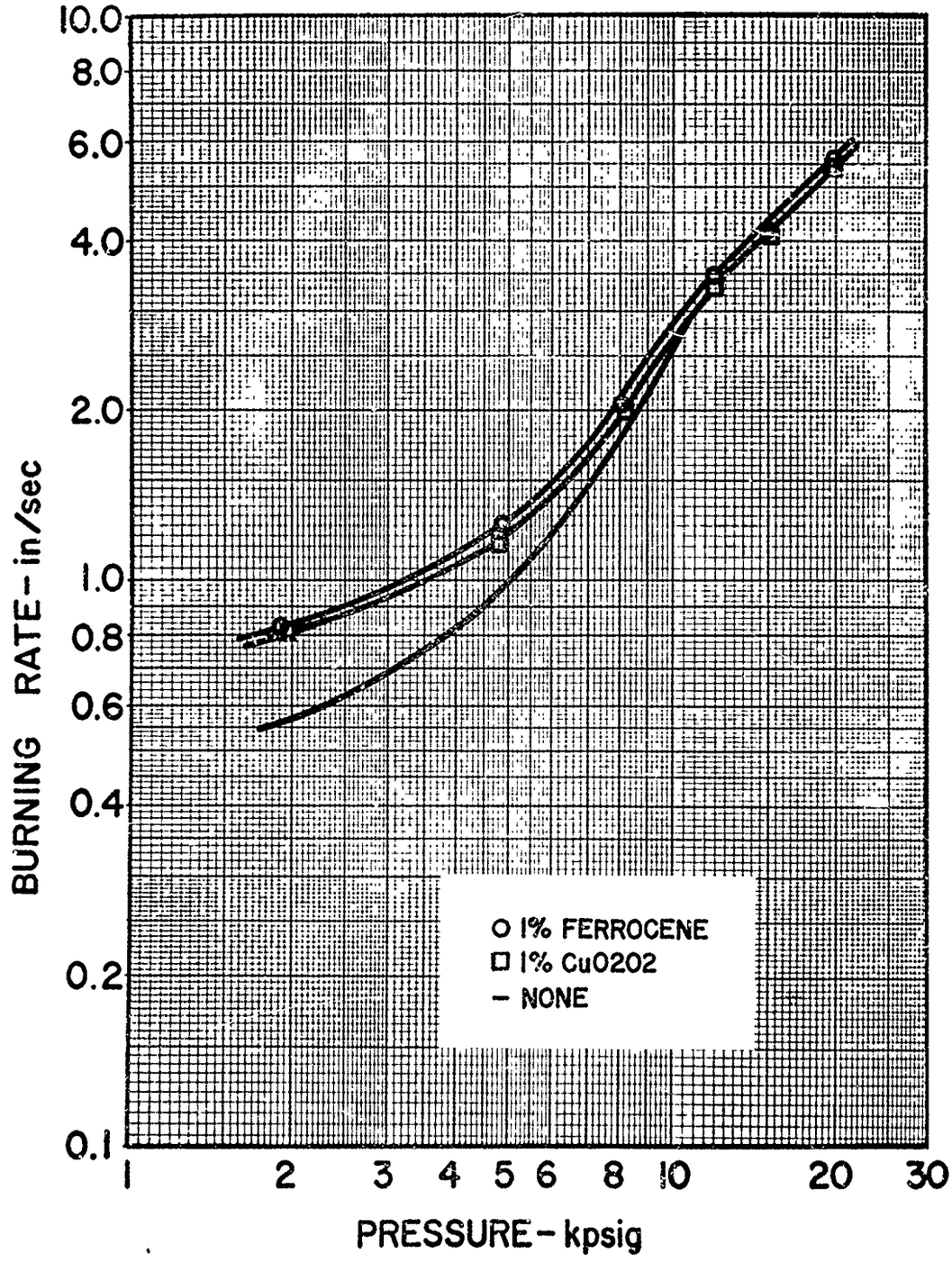

FIG. 19 Effect of Catalysts on High-Pressure Burning Rates of Inert-Binder Propellants ($\frac{1}{8}$-in. unrestricted strands) [1% ferrocene: RH-C-42ce; 1% Cu0202: RH-C-43ce; none: RH-C-40ce]

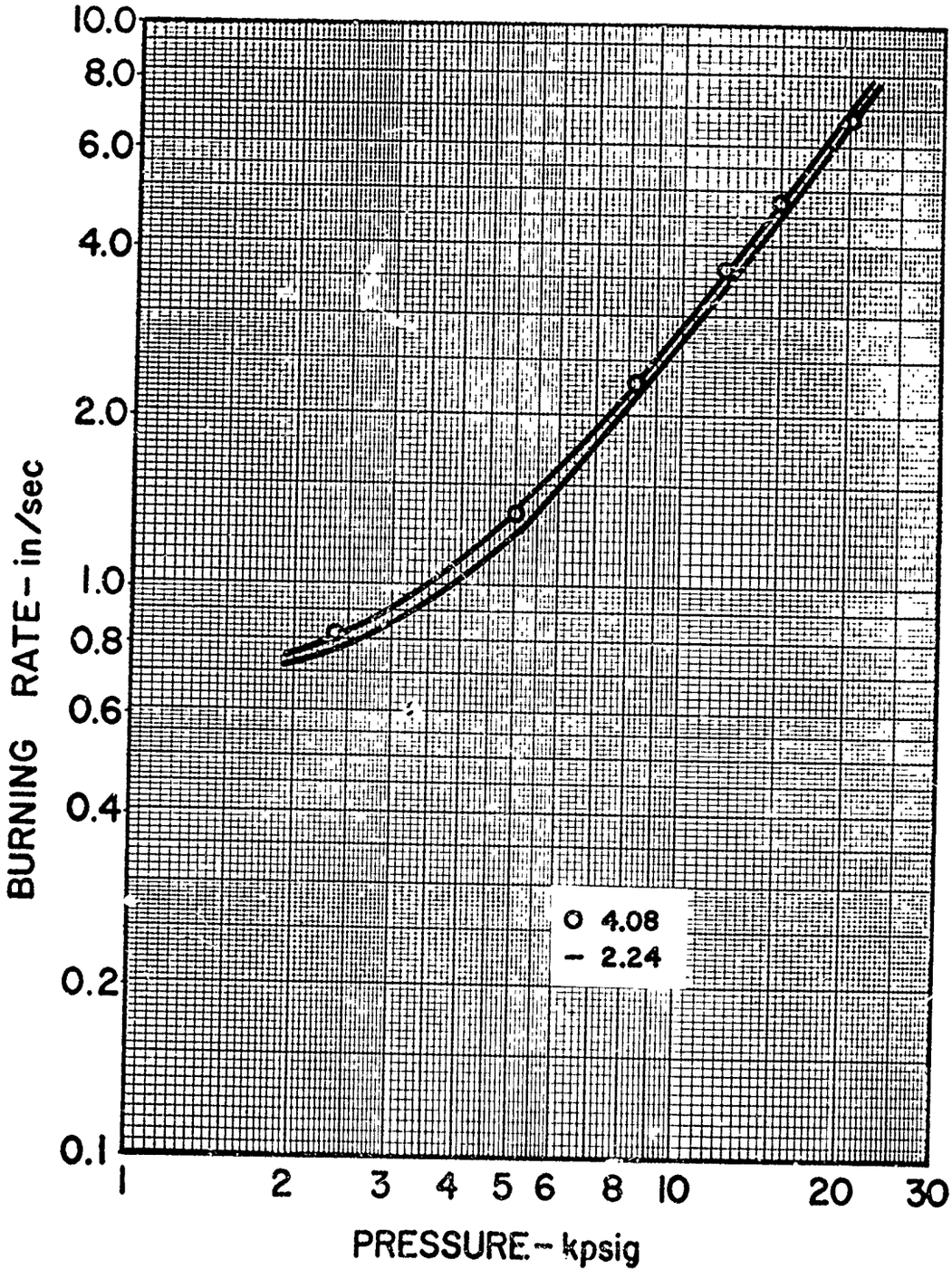

FIG. 20 Effect of Plasticizer/Double-Base-Powder Ratio on High-Pressure Burning Rates of Plastisol-Nitrocellulose Propellants ($\frac{1}{8}$-in. unrestricted strands)[4.08: RH-P-402cb; 2.24: RH-P-181cb]

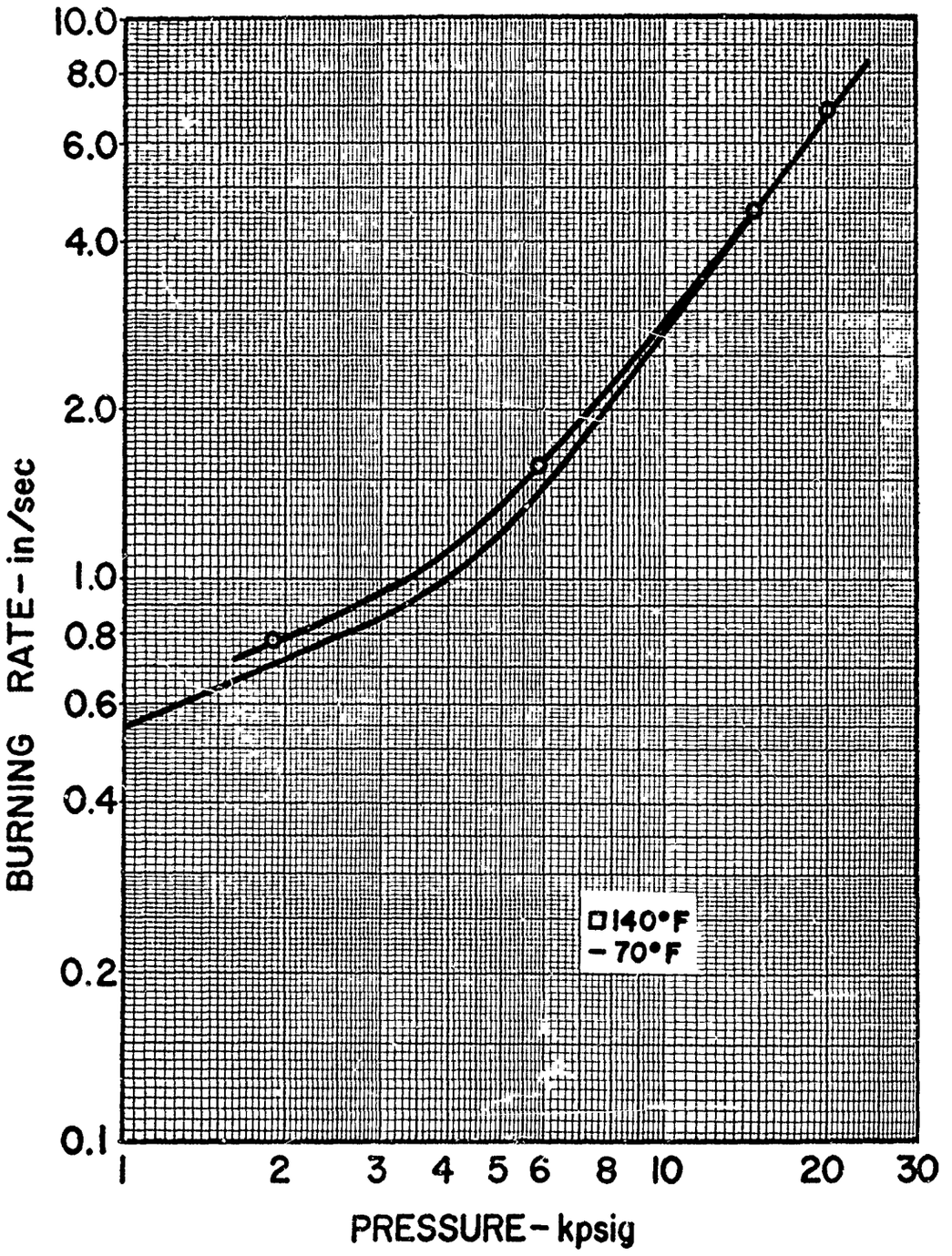

FIG. 21 Effect of High Conditioning Temperature on High-Pressure Burning Rate of Plastisol-Nitrocellulose Propellant ($\frac{1}{8}$-in. unrestricted strands)[RH-P-181cb]

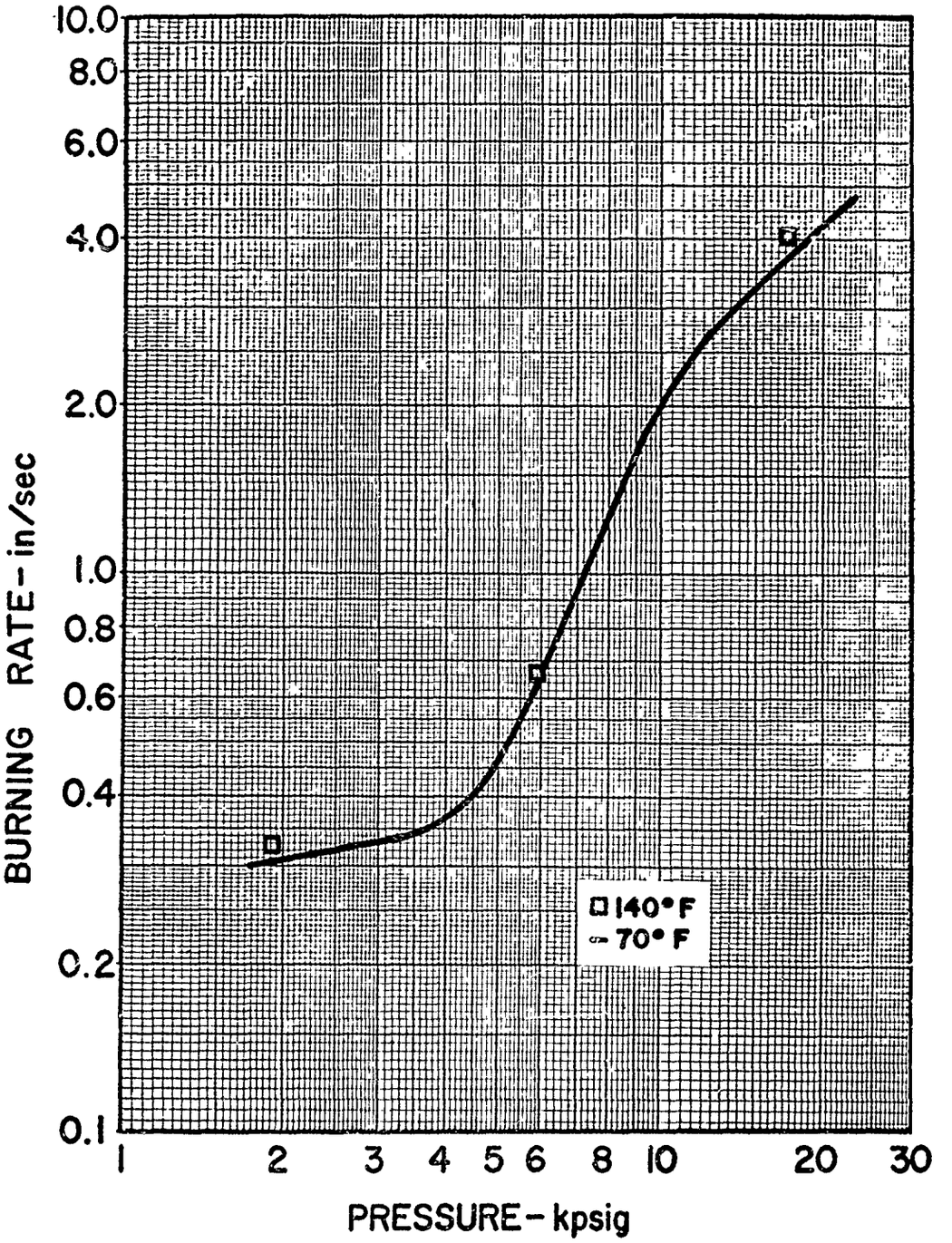

FIG. 22 Effect of High Conditioning Temperature on High-Pressure Burning Rate of Inert-Binder Propellant ($\frac{1}{8}$-in. unrestricted strands)[RH-C-40cc]

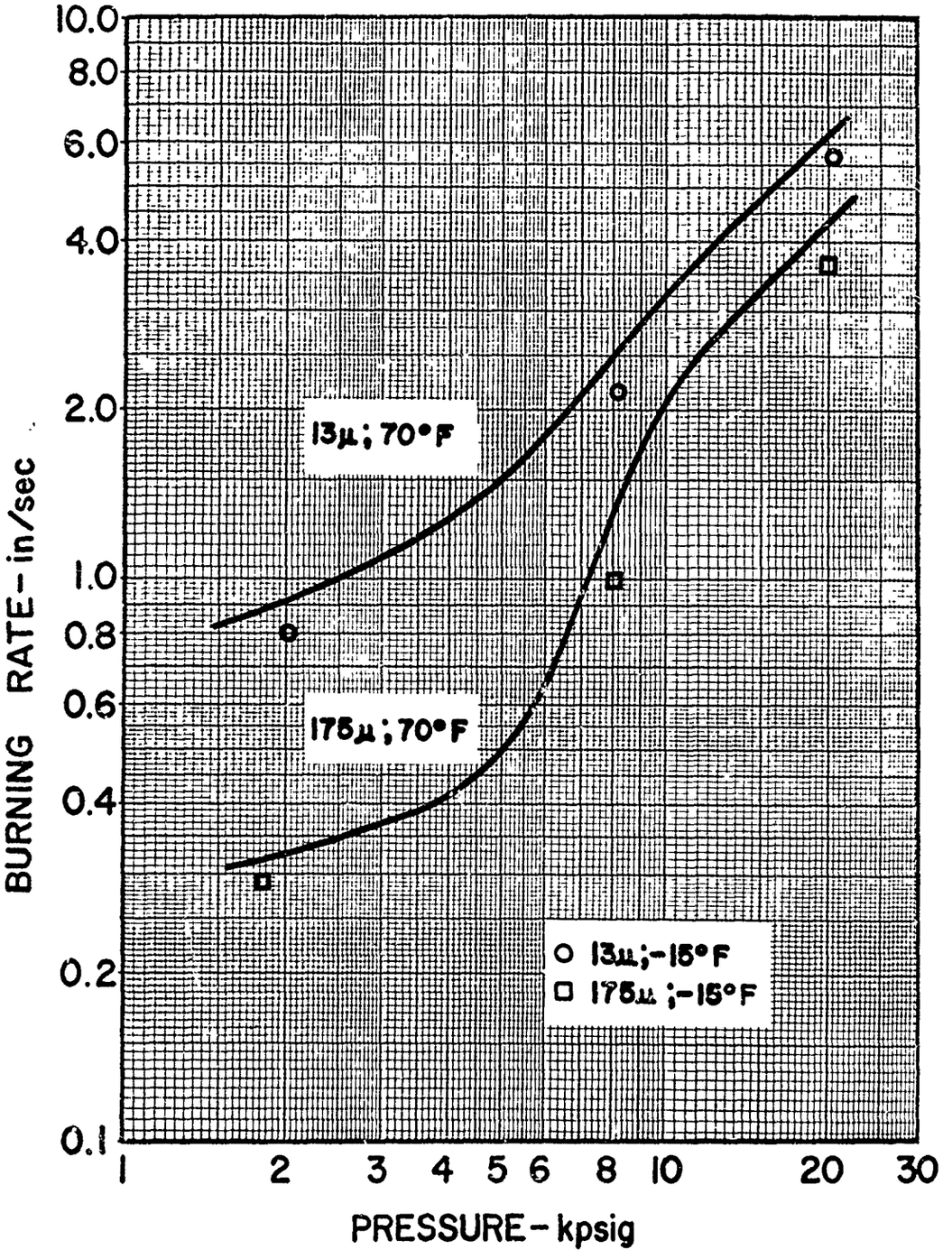

FIG. 23 Effect of Low Conditioning Temperature at Two Oxidizer-Particle Sizes on High-Pressure Burning Rates of Inert-Binder Propellants ($\frac{1}{8}$-in. strands) [13μ AP: RH-C-41ce; 175μ AP: RH-C-41cc]

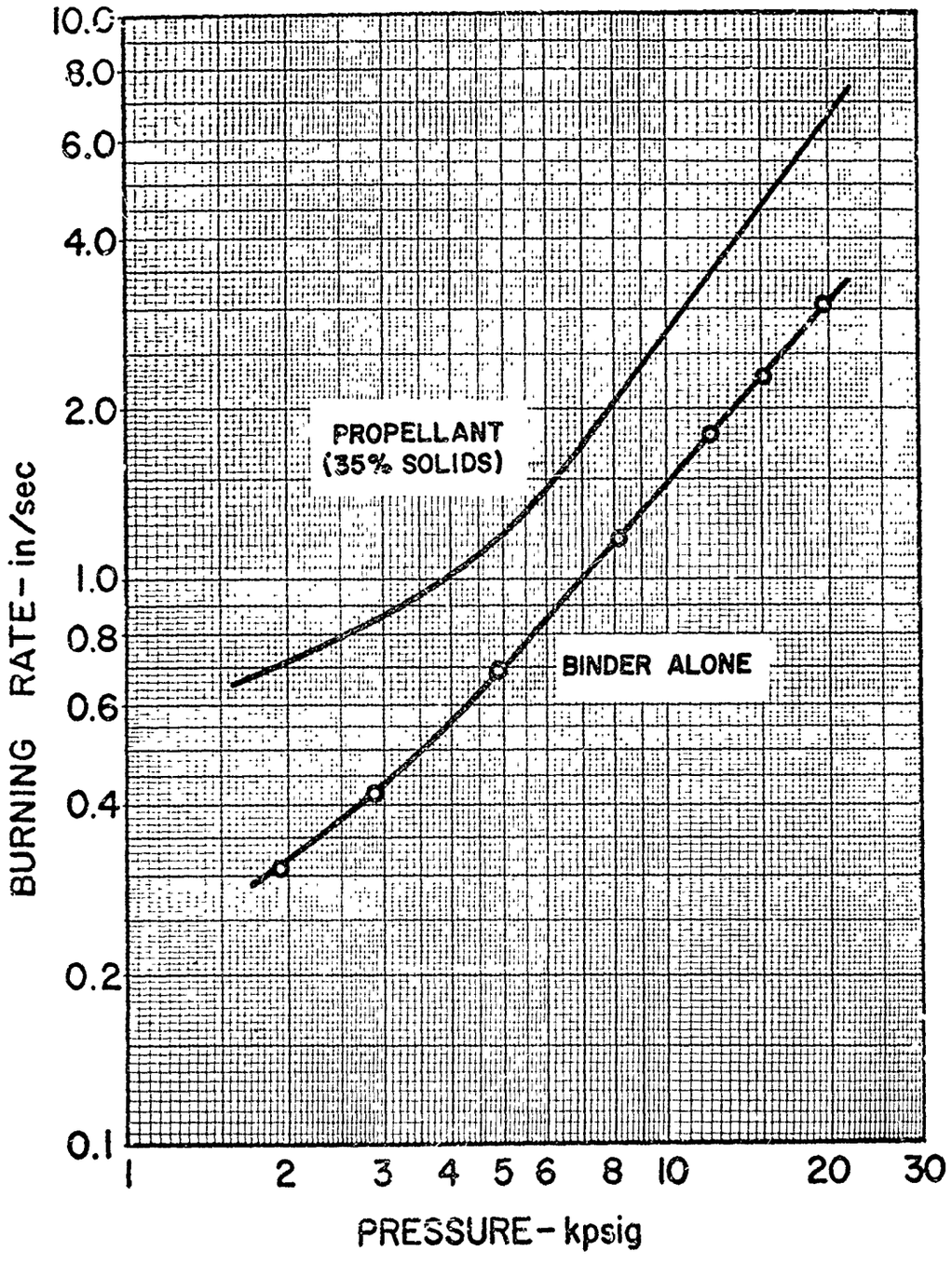

FIG. 24 High-Pressure Burning Rate of Plastisol-Nitrocellulose Binder [RH-P-181cb]

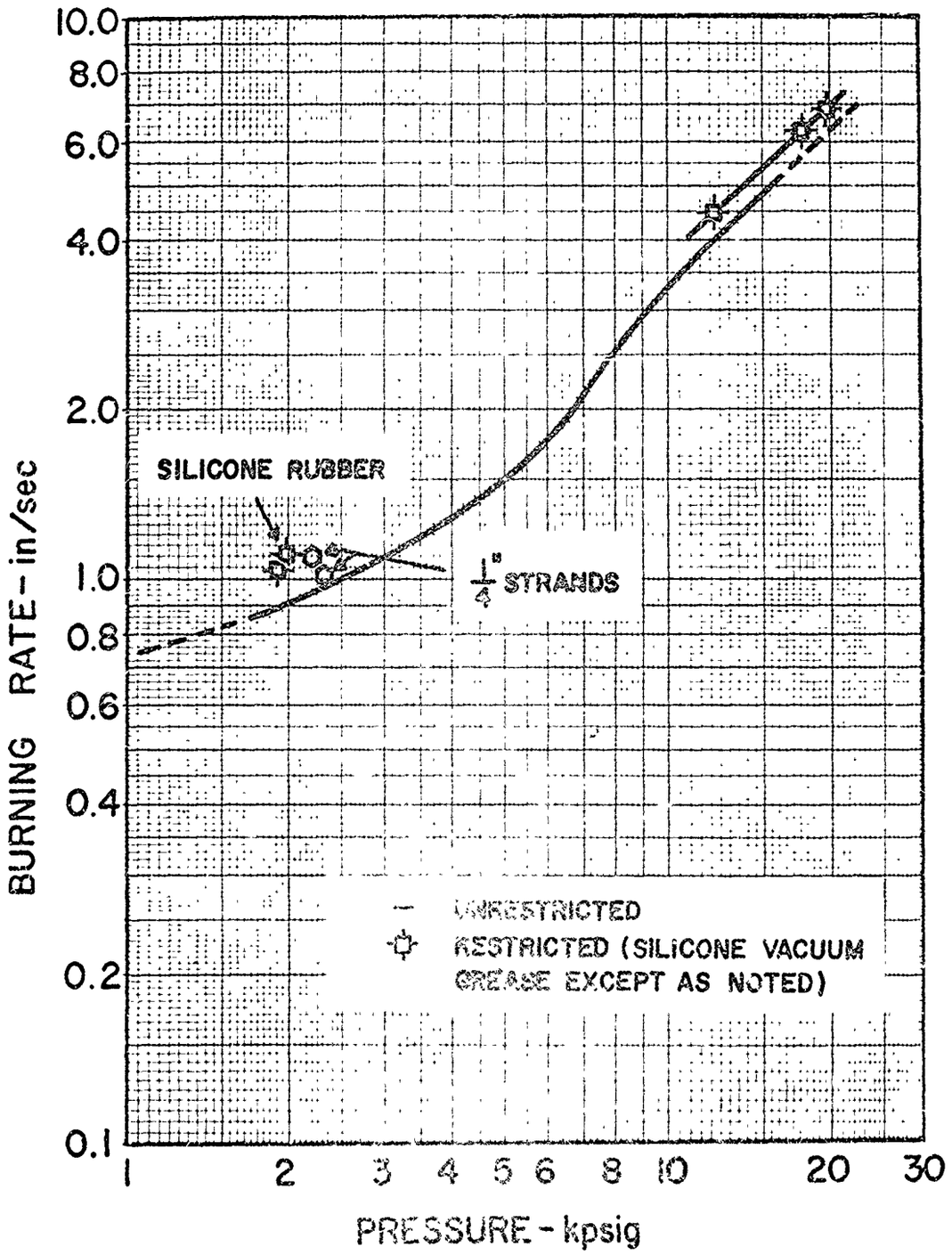

FIG. 25 Effect of Silicone-Containing Restrictors on High-Pressure Burning Rate of Inert-Binder Propellant ($\frac{1}{8}$-in. strands)[RH-C-41ce]

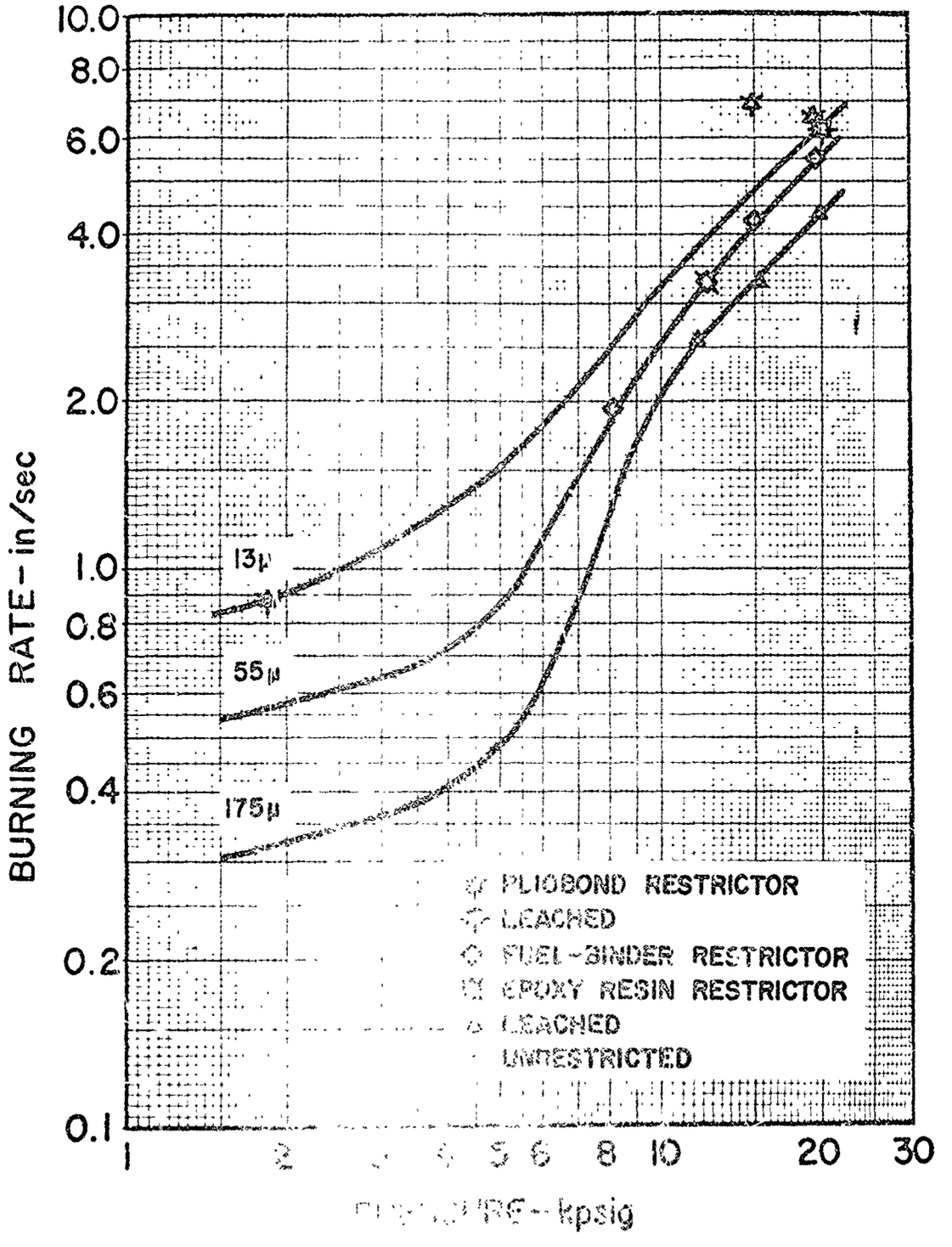

FIG. 26 Effects of Restriction and Surface Treatment on High-Pressure Burning Rate of Inert-Binder Propellant ($^1/_8$-in. strands) [RH-C-41cb, cc, and ce]

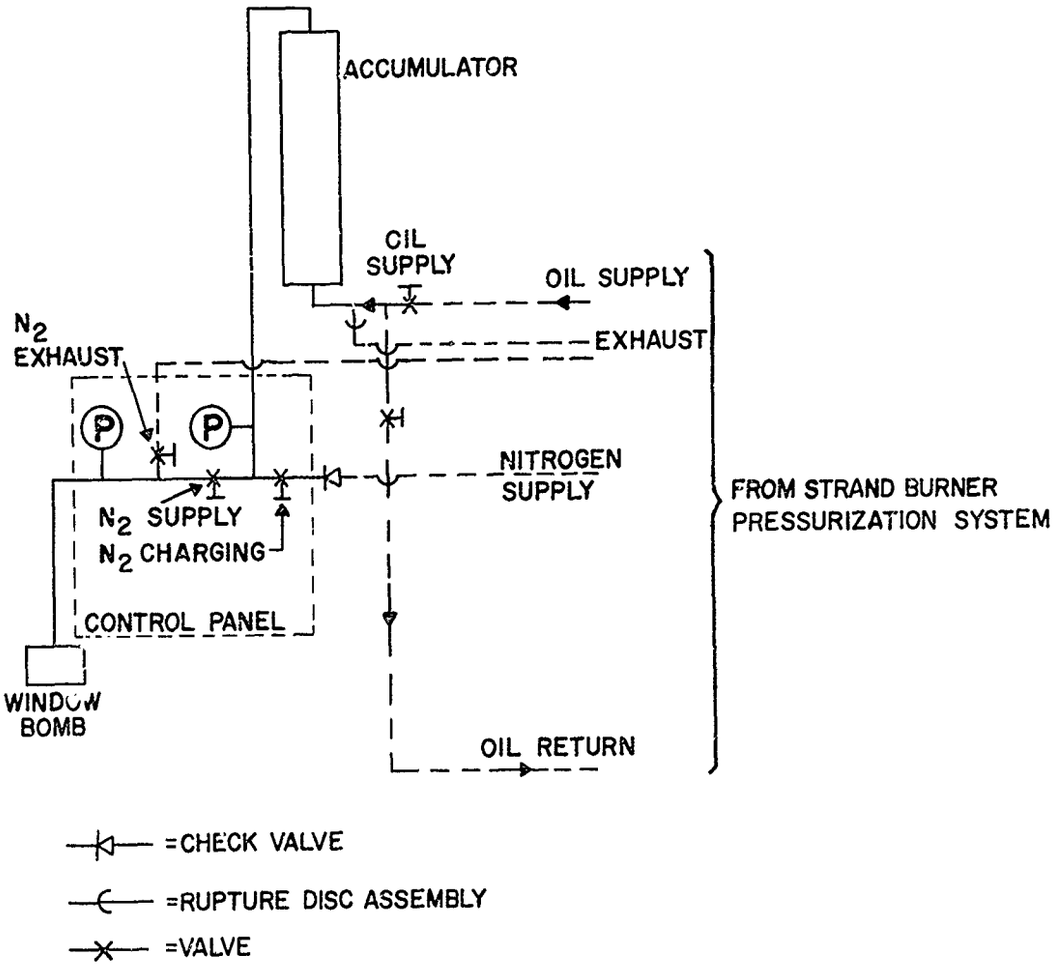

FIG. 27 Schematic Diagram of Micro-Window-Bomb Pressurization System

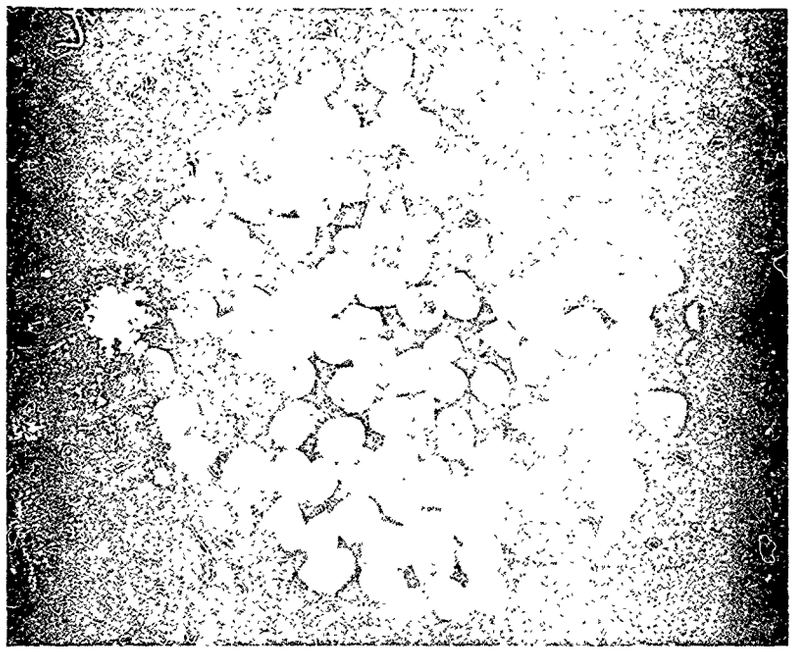

FIG. 28 Photomicrograph of Control Sample for Thermal-Shock Experiments on Ammonium Perchlorate Particles (diameters approx. 350μ; 12 × magnification)

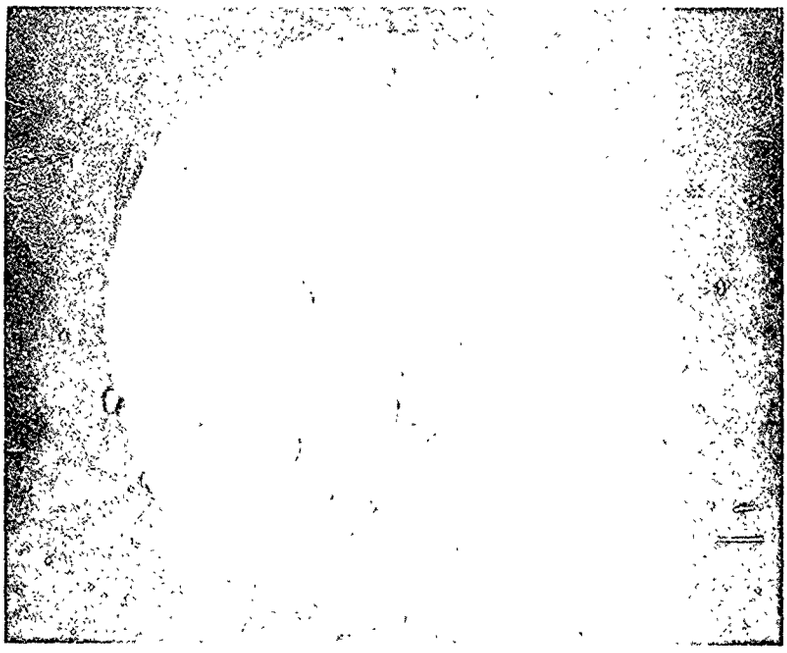

FIG. 29 Photomicrograph of Recovered Small Particles after Thermal-Shock Experiment (approx. 12 × magnification)

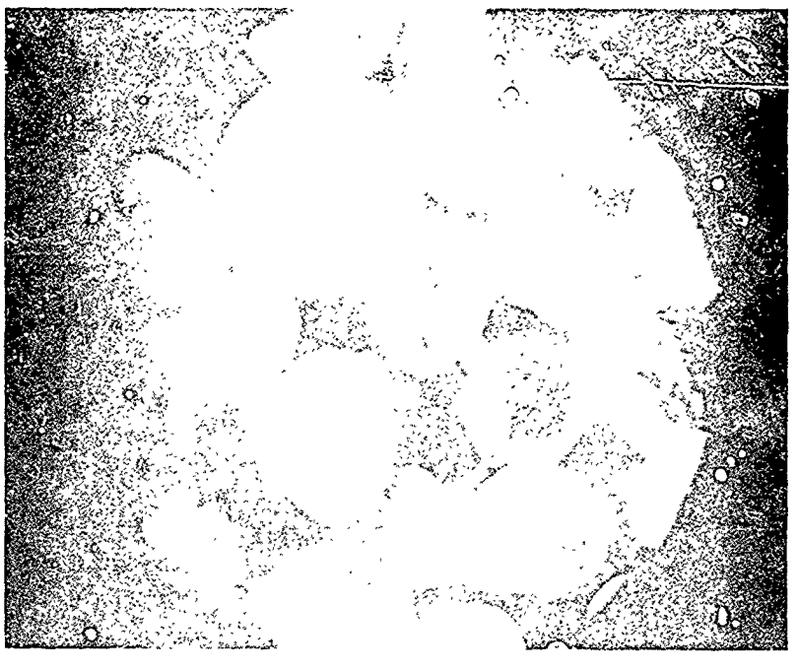

FIG. 30 Photomicrograph of Control Sample of Ammonium Perchlorate (diameters approx. 350μ; 40 × magnification)

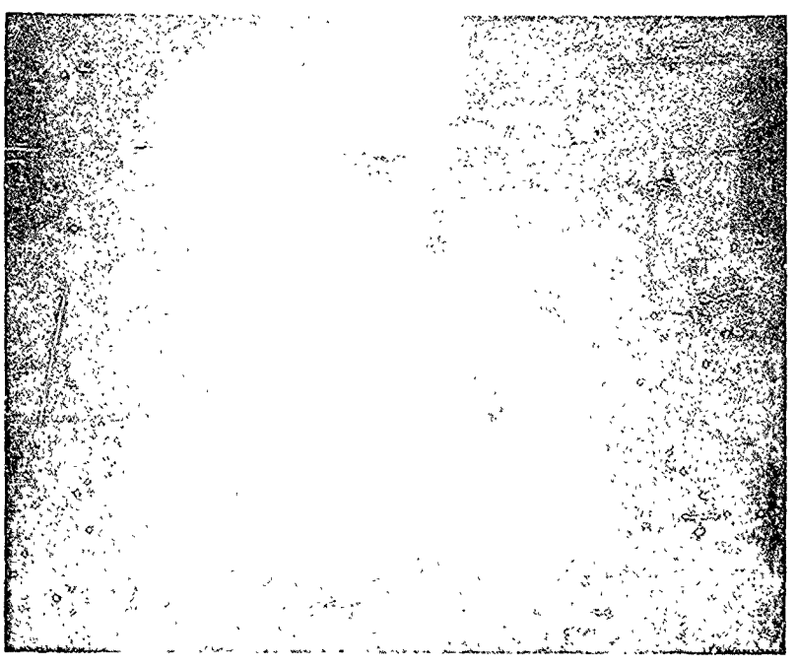

FIG. 31 Photomicrograph of Recovered Large Particles after Thermal-Shock Experiment (approx. 40 × magnification)

APPENDIX

EFFECTIVE COMBUSTION PRESSURE DURING BURNING IN A DYNAMIC PRESSURE ENVIRONMENT

I. General Derivation

Consider the one-dimensional regression of a burning solid propellant over a fixed distance, Δx, in a time, Δt. An average regression rate for the process may be measured:

$$\bar{r} \equiv \frac{\Delta x}{\Delta t} \tag{A-1}$$

Assume that a steady-state pressure-dependency function, $F[P]$, characterizes the effect of pressure on regression rate in a constant-pressure situation such that:

$$r \equiv F[P] \tag{A-2}$$

Considering a dynamic pressure situation with pressure a function of time, $P(t)$, then, in general, $r(t)$ may be less than, equal to, or greater than $F[P(t)]$ depending on the form of $P(t)$.

If it is assumed that the combustion pressure and, hence, the regression rate are changing quasi-steadily, then

$$r(t) = F[P(t)] \tag{A-3}$$

Then

$$\bar{r} \equiv \frac{\Delta x}{\Delta t} = \frac{\int_{\Delta t} F[P(t)]dt}{\Delta t}$$

and, consequently, if $F[P]$ and $P(t)$, as well as Δt, are known, an effective pressure, P^*, may be defined through the relation

$$\bar{r} = F[P^*] = \frac{\int_{\Delta t} F[P(t)]\,dt}{\Delta t} \qquad \text{(A-4)}$$

Assuming again that the dynamic pressure environment which combustion takes place results in quasi-steady combustion, then it is $\bar{r}$ and P^* which are properly reported as the regression-rate data of strand-burning experiments.

II. Case When the Regression Rate Law is Known

Presume that $F[P]$ is known. In this case, Eq. A-4 may be integrated using $P(t)$ data to determine P^*. In general, numerical integration would be required.

Consider, however, the classic regression-rate law,

$$r = AP^n \qquad \text{(A-5)}$$

where A is independent of pressure and n, the so-called "pressure index", is nearly constant, at least over a small pressure range. Then, from Eq. A-4,

$$\bar{r} = A(P^*)^n = \frac{\int_{\Delta t} A[P(t)]^n dt}{\Delta t} \qquad \text{(A-6)}$$

or

$$P^*(\bar{r}) = \left(\frac{\int_{\Delta t} [P(t)]^n dt}{\Delta t} \right)^{\frac{1}{n}} \qquad \text{(A-7)}$$

or, non-dimensionally)

$$\frac{P^*(\bar{r})}{P_o} = \int_o^1 [P(t)/P_o]^n d\tau \qquad \text{(A-8)}$$

where $\tau \equiv t/\Delta t$ and P_o is any convenient reference pressure characterizing the nominal pressure level of the experiment. Thus, from solution of Equation A-8, the value of P^* corresponding to the P(t) data of a given firing may be determined if n is known.

Strictly speaking, n is an unknown since it is part of the unknown form of $F[P] (=AP^n)$ which is the desired result of, say, strand-burning experiments. Raw strand-burner data may, however, be used to estimate n. Raw pressure data might, for example, be the initial or final burner pressures, their average, or some other pressure value characterizing the experiments. Raw regression rate data would be the measured value of $\bar{r}$. Calculated values of P^* using Eq. A-7 or A-8, and an estimated value of n may be used to redetermine n and allow iterative treatment of the pressure data to determine ultimately the correct P^* of the experiment.

III. Case When the Pressure Change is Linear in Time

It is assumed that:

$$P(t) = P(\tau) = P_1 + \tau \Delta P \qquad \text{(A-9)}$$

where P_1 is the pressure at time t_1 and ΔP is the pressure rise during the burning interval Δt ($P_2 \doteq P_1 + \Delta P$), then, from Eq. A-8 with P_o chosen as P_1,

$$\frac{P(\bar{r})^*}{P_1} = \left(\int (1 + P\tau)^n d\tau \right)^{\frac{1}{n}}$$

or

$$\frac{P(\bar{r})^*}{P_1} = \left(\frac{(1 + P)^{n+1} - 1}{(n+1)P} \right)^{\frac{1}{n}} \qquad \text{(A-10)}$$

where $P \equiv \Delta P/P_1$

In the event that n = 1, it may be readily shown that

$$P^*(\bar{r},\ n = 1) = \frac{P_1 + P_2}{2} \equiv \overline{P} \qquad \text{(A-11)}$$

Hence, the arithmetic mean pressure of burning, $\overline{P}$, may be expected to be a reasonable approximation to P^* when $n \cong 1$. Since the usual range of values for n for solid propellants (even at high pressures) is about $0.2 \leqq n \leqq 2.0$, a more useful expression than Eq. A-10 above is

$$\frac{P^*}{\overline{P}} = \left(\frac{(1+P)^{n+1} - 1}{(n+1)P\left(\frac{P}{2}\right)^n} \right)^{\frac{1}{n}} \qquad \text{(A-12)}$$

which results from substituting Eq. A-13,

$$P_1 = \frac{\overline{P}}{1 + \frac{P}{2}} \qquad \text{(A-13)}$$

into Eq. A-10. As should be expected, Eq. A-12 reduces to $P^*/\overline{P} = 1$ for n = 1.

In the event that $n \neq 1$, Eq. A-12 is a useful one for predicting the error involved in assuming $P^* = \overline{P}$, this assumption being a convenient one for the reduction of strand-burning data to r—P plots.

As an approximation to Eq. A-12, for small values of P it may be shown that

$$\frac{P^*}{\overline{P}} \cong 1 + \frac{n-1}{24} P^2 \qquad \text{(A-14)}$$

This approximation is achieved by expressing Eq. A-12 as an infinite power series in the variable P, i.e.,

$$\frac{P^*}{\overline{P}} = (1 + c_1 P + c_2 P^2 + \ldots)^{\frac{1}{n}} \qquad \text{(A-15)}$$

where it may be shown that:

$$c_1 = 0$$

$$c_2 = n(n-1)\left(\frac{1}{3!} - \frac{1}{2!2^2}\right)$$

$$c_3 = n(n-1)\left[(n-2)\left(\frac{1}{4!} - \frac{1}{3!2^3}\right) - \left(\frac{1}{3!} - \frac{1}{2!2^2}\right)\frac{n}{1!2}\right]$$

etc.

Thus,

$$\frac{P^*}{\overline{P}} = 1 + \frac{1}{n}(n)(n-1)\left(\frac{1}{3!} - \frac{1}{2!2^2}\right) P^2 + (\text{terms of order } P^3 \text{ or less})$$

which leads to Eq. A-14. The absence of a first-order term ($c_1 = 0$) in Eq. A-15 is significant; it is a consequence of the choice of $\overline{P}$ as an approximation to P^*. Other approximations would, in general, introduce a first-order term into Eq. A-15 and hence into Eq. A-14.

III. Case of the 20,000 psig Oil-Filled Strand Burner

From the previous analysis it is clear that the major variables influencing the inaccuracy of pressure measurement introduced by pressure-averaging are first, the total fractional pressure rise, $P = \Delta P/P_1$ and the pressure index of the propellant, n. Additionally,

the absolute magnitude of the regression rate interplays with the time-rate-of-pressure in strand burning to determine whether the foregoing analysis is valid, i.e., whether combustion is, in fact, quasi-steady or not. The relatively low rates-of-pressure-rise encountered in the 20,000-psi strand burner (16,000 psi/sec maximum) probably are sufficient to validate this quasi-steady assumption.

The fractional error in P implied by assuming $\overline{P}$ equal to P^* for strand-burning experiments is shown approximately (to second order in $P = \Delta P/P_1$) in Figs. A-1 and A-2 where values calculated from Eq. A-14 are shown. Eq. A-14 may be shown to provide an overestimate of the fractional error, $P^*/\overline{P} - 1$. Several points typical of those extreme values of P and n encountered in the 20,000-psig strand burner are also shown in these Figures.

There is an additional, similar source of error in r—P data from strand burners operating with variable pressure during burning. This is the error introduced by pressure-averaging if the pressure index, n, is not independent of pressure. If it is not, Eq. A-6 and the relations derived from it are not strictly valid. It is probable, however, that, for the values of the fractional pressure rise, P, encountered in the experiments described elsewhere in this report, n is reasonably close to being constant over the range of pressures during each individual firing of the burner.

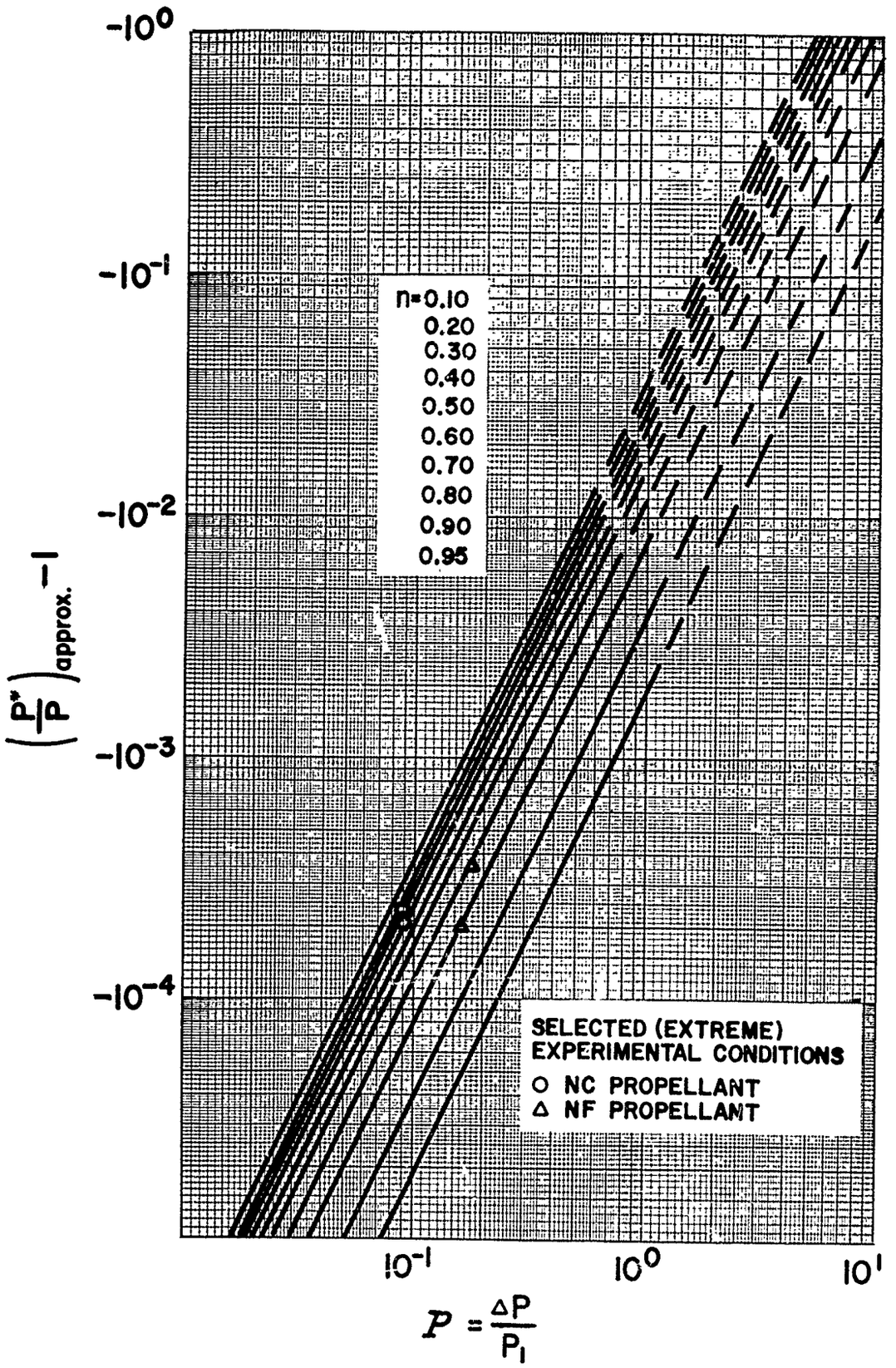

FIG. A-1 Fractional Pressure Averaging Error for n < 1

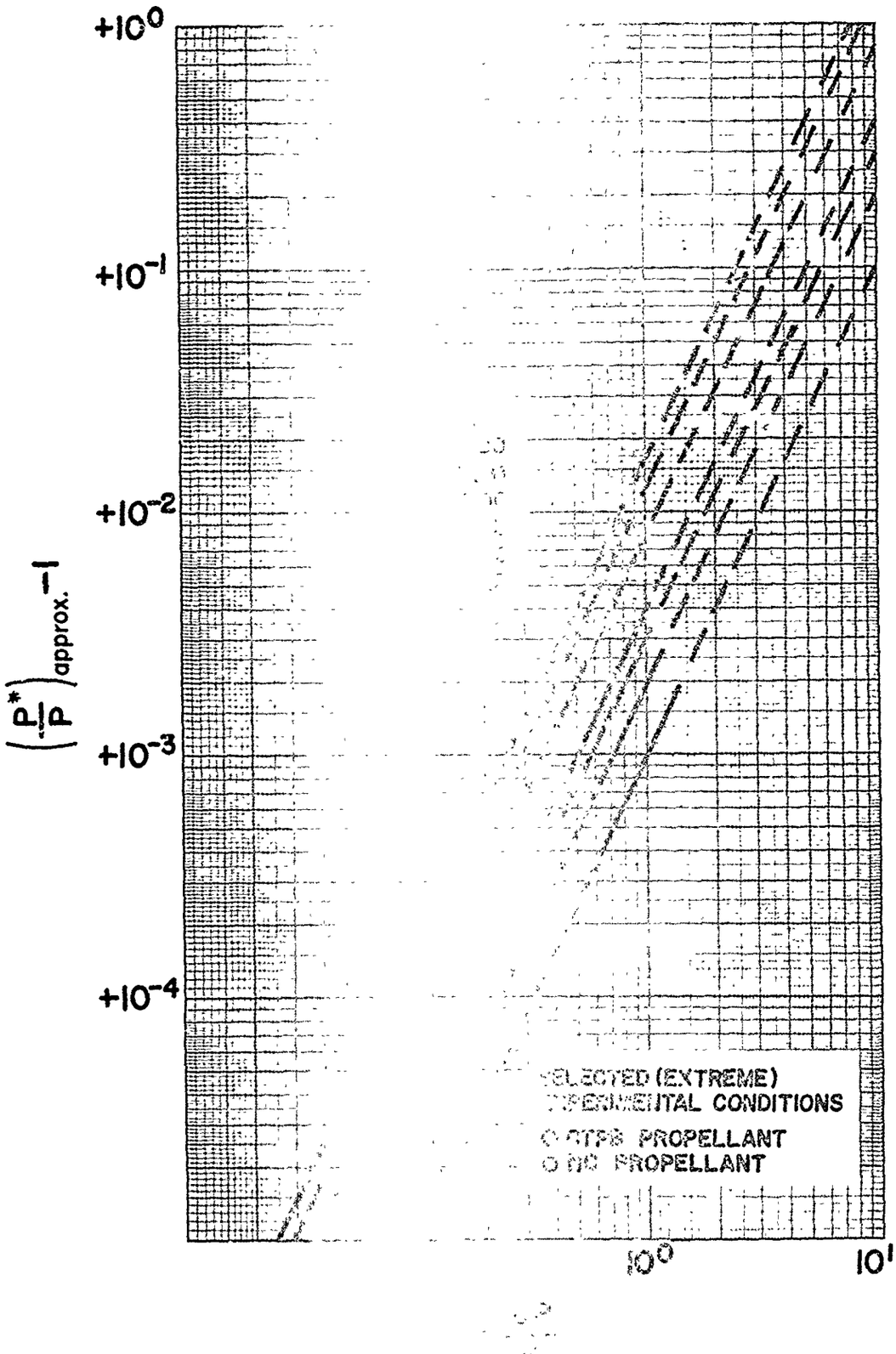

FIG. A-2 Fractional Pressure Averaging Error for $n > 1$

Initial distribution of this report has been made in accordance with "Chemical Propulsion Mailing List", CPIA Publication 74, March 1965 and approved supplements.

Qualified users may obtain this report from the Defense Documentation Center.

In addition to security requirements which must be met, this document is subject to special export controls and each transmittal to foreign governments or foreign nationals may be made only with prior approval of

Department of Army
Headquarters, U. S. Army Missile Command
Redstone Arsenal, Alabama 35809